

One-loop matching for leading-twist generalised transverse-momentum-dependent distributions

Valerio Bertone^{1*}, Miguel G. Echevarria^{2,3†}, Oscar del Rio^{4‡}, Simone Rodini^{5§}

¹*IRFU, CEA, Université Paris-Saclay, F-91191 Gif-sur-Yvette, France.*

²*Department of Physics, University of the Basque Country UPV/EHU, 48080 Bilbao, Spain.*

³*EHU Quantum Center, University of the Basque Country UPV/EHU.*

⁴*Department of Theoretical Physics & IPARCOS,
Complutense University of Madrid, 28040 Madrid, Spain.*

⁵*Deutsches Elektronen-Synchrotron DESY, Notkestr. 85, 22607 Hamburg, Germany.*

Abstract

We present the one-loop matching coefficients necessary to match all of the leading-twist generalised transverse-momentum-dependent distributions (GTMDs) onto generalised parton distributions (GPDs). Matching functions are extracted by computing the first radiative corrections to partonic bilocal correlators with staple-like Wilson lines, as appropriate for high-energy collisions. These correlators are characterised by a transverse displacement and skewed kinematics of external states. Using the proton helicity basis, they are parametrised in terms of GTMDs, which are subsequently related to leading-twist GPDs. Our results provide new insights into the complex dynamics of GTMDs generated by radiative corrections. In particular, we show that time-reversal even and odd contributions to GTMDs in the so-called ERBL region mix both under matching and evolution. Finally, we present a selection of numerical results and comment on the quantitative behaviour of GTMDs.

*valerio.bertone@cea.fr

†miguel.garciae@ehu.eus

‡oscar03@ucm.es

§simone.rodini@desy.de

Contents

1	Introduction	2
2	Definitions and conventions	3
3	Matching functions	4
4	Matching for specific parametrisations	9
5	Reconstructing GTMDs	12
6	Numerical results	15
7	Conclusions	17
A	On the presence of imaginary contributions	18
A.1	Imaginary part in the evolution	18
A.2	Imaginary part in the residual function	20
A.3	Vanishing imaginary part in the splitting functions	21
B	Fourier transformation	22

1 Introduction

A key ingredient in all modern phenomenological extractions of transverse-momentum-dependent distributions (TMDs) [1–9] is a set of perturbative matching coefficients that encode the operator product expansion of TMD operators in terms of collinear light-cone operators [10, 11]. On the theoretical side, this set of relations must be satisfied by realistic models. On the phenomenological side, these relations allow for simpler modeling and reduce parametric freedom of input models, thus increasing quality and time requirements for extractions of TMDs from experimental data.

In the case of forward TMDs, which are involved in inclusive processes, a wealth of perturbative knowledge is currently available for the leading-twist matching coefficients [11–26] and some information for the next-to-leading-twist matching coefficients [27–29]. In contrast, in the case of non-forward TMDs, a.k.a. generalised TMDs (GTMDs), very little perturbative information is currently available [30]. GTMDs have been introduced and formalised in Refs. [31–35] and one of their most interesting aspects is their ability to give access to the orbital angular momentum of quarks [36–39]. Although several proposals to probe GTMDs have been put forward in recent years (see, , *e.g.*, Refs. [40–49]) and a proof of factorisation has recently been obtained [50], GTMDs remain elusive objects, very challenging to access experimentally due to the exclusive nature of the processes they are involved in. In order to perform any exploratory study of their phenomenological impact, it is essential to have a solid theoretical foundation, so that relevant details are not washed away by model freedom.

Our aim with this work is to present the complete set of one-loop, *i.e.* $\mathcal{O}(\alpha_s)$, corrections to the matching relations between leading-twist GTMDs and generalised parton distributions (GPDs) by completing, expanding, and to some extent amending the work of Ref. [30]. Going beyond $\mathcal{O}(\alpha_s)$ is, at present, a superfluous step, which is computationally very intensive due to the non-forward nature of GTMDs. Going beyond leading-twist accuracy is similarly superfluous, as it would produce a set of matching relations that involve a large number of completely unknown twist-three GPDs. Therefore, for the foreseeable future, the only potentially relevant matching coefficients are those presented in this work.

The work is organised as follows: in Sec. 2, we summarise all relevant definitions and conventions used in the paper; in Sec. 3, we present the results for the matching coefficients and, in Sec. 4, we construct the matching on GPDs for all twist-two GTMDs in a given parametrisation.

In Sec. 5, we provide the master formula for matching and evolution, which we use in Sec. 6 to present numerical results. In Sec. 7, we draw our conclusions.

2 Definitions and conventions

We start by introducing two light-cone vectors, n and \bar{n} , defined in a way that $n^2 = \bar{n}^2 = 0$ and $(\bar{n}n) = 1$,¹ and which define the longitudinal plane. The transverse plane orthogonal to n and \bar{n} is parametrised by two additional vectors, R and L , which satisfy the following orthonormality conditions:

$$R^2 = L^2 = (Rn) = (Ln) = (R\bar{n}) = (L\bar{n}) = 0, \quad (RL) = -1. \quad (1)$$

With this basis of vectors at hand, any generic four-vector v can be decomposed as $v = v^+\bar{n} + v^-n - v_R L - v_L R$, where $v^+ = (vn)$, $v^- = (v\bar{n})$, $v_R = (vR)$ and $v_L = (vL)$. An explicit implementation of the basis vectors is given by:

$$\begin{aligned} n^\mu &= \frac{1}{\sqrt{2}}(1, 0, 0, -1), & \bar{n}^\mu &= \frac{1}{\sqrt{2}}(1, 0, 0, 1), \\ R^\mu &= -\frac{1}{\sqrt{2}}(0, 1, i, 0), & L^\mu &= -\frac{1}{\sqrt{2}}(0, 1, -i, 0). \end{aligned} \quad (2)$$

The scalar product between the generic vector v and a purely transverse vector w_T , *i.e.* a four-vector characterised by $w_T^+ = w_T^- = 0$, produces $(vw_T) = -\mathbf{v} \cdot \mathbf{w}_T$, where the r.h.s. denotes the scalar product between two two-dimensional vectors in Euclidean space. Moreover, given any generic tensor $T^{\mu_1\mu_2\dots}$, we will use the following shorthand notation for its contraction with the four-vectors $a_{\mu_1}, b_{\mu_2}, \dots$: $a_{\mu_1} b_{\mu_2} \dots T^{\mu_1\mu_2\dots} \equiv T^{ab\dots}$.

We now turn to the definition of the partonic correlators that we will use to extract the matching coefficients. The relevant quark and gluon GTMD correlators read:

$$\begin{aligned} \mathcal{F}_{q/H}^{[Y]}(x, \xi, \mathbf{b}, \Delta_T) & \quad (3) \\ &= S_q^{-\frac{1}{2}}(\mathbf{b}) \int \frac{dz}{2\pi} e^{-ixp^+z} \left\langle p + \frac{\Delta}{2}, \lambda' \left| \bar{\psi}_i \left(\frac{zn}{2} + \frac{\mathbf{b}}{2} \right) Y_{ij} \mathcal{W}_s \psi_j \left(-\frac{zn}{2} - \frac{\mathbf{b}}{2} \right) \right| p - \frac{\Delta}{2}, \lambda \right\rangle, \end{aligned}$$

$$\begin{aligned} \mathcal{F}_{g/H}^{[Y]}(x, \xi, \mathbf{b}, \Delta_T) & \quad (4) \\ &= S_g^{-\frac{1}{2}}(\mathbf{b}) \int \frac{dz}{2\pi} \frac{e^{-ixp^+z}}{xp^+} \left\langle p + \frac{\Delta}{2}, \lambda' \left| F^{\mu\nu} \left(\frac{zn}{2} + \frac{\mathbf{b}}{2} \right) Y_{\mu\nu} \mathcal{W}_s F^{\nu\mu} \left(-\frac{zn}{2} - \frac{\mathbf{b}}{2} \right) \right| p - \frac{\Delta}{2}, \lambda \right\rangle, \end{aligned}$$

where $p - \Delta/2$ and λ ($p + \Delta/2$ and λ') denote momentum and helicity of the incoming (outgoing) hadron H , respectively. As usual, x is the fraction of momentum p along the longitudinal direction carried by the parton (q or g); while $\xi = -(\Delta n)/2(pn)$, a.k.a. skewness parameter, is the fraction of the momentum transfer Δ w.r.t. p along the longitudinal direction. ψ_j is the j -th component of the Dirac spinor for the quark q , and $F^{\mu\nu} = t_a F_a^{\mu\nu}$, with $F_a^{\mu\nu}$ the gluon field strength for colour configuration a and t_a the corresponding SU(3) group generator. In both correlators, the bilocal operator is characterised by the transverse displacement \mathbf{b} . Therefore, the variables x, ξ, \mathbf{b} , and Δ_T , *i.e.* the transverse component of Δ , fully define the kinematics of the correlator. \mathcal{W}_s is the staple-like Wilson line which connects the two space-time points of the bilocal operator and which runs along the light-cone direction defined by n up to $s\infty$, where the sign $s = \pm 1$ depends on the process under consideration. The colour representation of the Wilson line is the fundamental one for the quark correlator and the adjoint one for the gluon correlator. Important ingredients of the definitions in Eqs. (3) and (4) are the soft functions S_i , with $i = q, g$, whose presence is necessary to ensure the cancellation of the so-called rapidity divergences generated by the partonic correlators [30, 35]. S_i is a universal perturbative quantity currently known up to three-loops in perturbative QCD [51]. In this work, we will only need the one-loop result.

¹Scalar products between four-vectors in Minkowski space are expressed as $a^\mu b_\mu \equiv (ab)$.

The corresponding operator definitions for quark and gluon GPD correlators are:

$$F_{q/H}^{[\Gamma]}(x, \xi, \Delta_T) = \int \frac{dz}{2\pi} e^{-ixp^+z} \left\langle p + \frac{\Delta}{2}, \lambda' \left| \bar{\psi}_i \left(\frac{zn}{2} \right) \Gamma_{ij} \mathcal{W} \psi_j \left(-\frac{zn}{2} \right) \right| p - \frac{\Delta}{2}, \lambda \right\rangle, \quad (5)$$

$$F_{g/H}^{[\Gamma]}(x, \xi, \Delta_T) = \int \frac{dz}{2\pi} \frac{e^{-ixp^+z}}{xp^+} \left\langle p + \frac{\Delta}{2}, \lambda' \left| F^{\mu+} \left(\frac{zn}{2} \right) \Gamma_{\mu\nu} \mathcal{W} F^{\nu+} \left(-\frac{zn}{2} \right) \right| p - \frac{\Delta}{2}, \lambda \right\rangle, \quad (6)$$

which are obtained from the GTMD correlators in Eqs. (3) and (4) by setting $\mathbf{b} = 0$ (which also implies that the soft functions S_i reduce to unity). Because of the vanishing transverse displacement, the Wilson line \mathcal{W} no longer depends on the light-cone direction, hence we dropped the subscript s .

Finally, we define the projectors Y and Γ that enter into the definitions of the GTMD and GPD correlators, respectively, and which run over the same set of Dirac (for quarks) and Lorentz (for gluons) structures. They are given by:²

$$\text{quarks : } Y_{ij}, \Gamma_{ij} \in \left\{ \frac{\gamma^+}{2}, \frac{\gamma^+ \gamma_5}{2}, \frac{i\sigma^{R+} \gamma_5}{\sqrt{2}} \right\}_{ij}, \quad (7)$$

$$\text{gluons : } Y^{\mu\nu}, \Gamma^{\mu\nu} \in \left\{ -g_T^{\mu\nu}, -i\varepsilon_T^{\mu\nu}, 2R^\mu R^\nu \right\}, \quad (8)$$

where:

$$g_T^{\mu\nu} = g^{\mu\nu} - n^\mu \bar{n}^\nu - n^\nu \bar{n}^\mu = R^\mu L^\nu + R^\nu L^\mu, \quad (9)$$

$$\varepsilon_T^{\mu\nu} = \varepsilon^{\mu\nu \bar{n} n} = R^\mu L^\nu - R^\nu L^\mu, \quad (10)$$

with $\varepsilon_T^{12} = +1$. The projectors in Eqs. (7) and (8) are engineered to project out the *leading-twist* (twist-two) parts of the correlators. Specifically, we have that: $\gamma^+/2$ and $-g_T^{\mu\nu}$ project out the unpolarised (U) components, $\gamma^+ \gamma_5/2$ and $-i\varepsilon_T^{\mu\nu}$ project out the longitudinally-polarised (L) components, and $i\sigma^{R+} \gamma_5/\sqrt{2}$ and $2R^\mu R^\nu$ project out the transversely(quark)/linearly(gluon) polarised (T) components. Note that we use the letter L both as a label for longitudinal polarisations and as one of the two basis vectors for the transverse space. The meaning of each instance of L should however be clear from context.

3 Matching functions

According to the operator-product expansion (OPE) formalism [10, 11, 20], the GTMD correlators in Eqs. (3) and (4) at small $|\mathbf{b}|$ can be expanded in terms of correlators characterised by light-like separations which can be identified with the GPD correlators in Eqs. (5) and (6). The OPE leading term for GTMD correlators can thus be factorised as:

$$\begin{aligned} \mathcal{F}_{i/H}^{[Y]}(x, \xi, \mathbf{b}, \Delta_T; \mu, \zeta) &= \int_x^\infty \frac{dy}{y} C_{i/j}^{Y/\Gamma}(y, \kappa, \mathbf{b}; \mu, \zeta) F_{j/H}^{[\Gamma]} \left(\frac{x}{y}, \xi, \Delta_T; \mu \right) \\ &\equiv \left[C_{i/j}^{Y/\Gamma} \otimes F_{j/H}^{[\Gamma]} \right] (x, \xi, \mathbf{b}, \Delta_T; \mu, \zeta), \end{aligned} \quad (11)$$

where repeated flavour (j) and polarisation (Γ) indices are implicitly summed over. An important feature of Eq. (11) is that the matching functions $C_{i/j}^{Y/\Gamma}$ are generally not diagonal in polarisation space. This implies that, for any given GTMD polarisation Y , GPDs with different polarisations Γ can contribute to it through matching.

We notice that the matching functions $C_{i/j}^{Y/\Gamma}$ can only depend over ξ through the ratio:

$$\kappa = \frac{\xi}{x}. \quad (12)$$

²Projectors obtained through the replacement $R \rightarrow L$ project out the same GTMD/GPD correlators, hence need not be considered separately.

Importantly, by separating the correlators into their even and odd contributions under $x \rightarrow -x$, it is always possible to reduce ourselves to considering $\kappa > 0$.³ We also introduced the scales μ and ζ which emerge from the renormalisation of the UV and rapidity divergences of the correlators, respectively. For the exact definition of the rapidity scale ζ we refer to App. A.

The functions $C_{i/j}^{Y/\Gamma}$ admit the following power-series expansion in terms of the strong-coupling constant α_s :

$$C_{i/j}^{Y/\Gamma}(y, \kappa, \mathbf{b}; \mu, \zeta) = \delta_{ij} \delta_{Y\Gamma} \delta(1-y) + \sum_{n=1}^{\infty} \left(\frac{\alpha_s(\mu)}{4\pi} \right)^n C_{i/j}^{Y/\Gamma, [n]}(y, \kappa, \mathbf{b}; \mu, \zeta). \quad (13)$$

In the following, we will compute the one-loop contributions to this expansion, *i.e.* $C_{i/j}^{Y/\Gamma, [1]}$, which can be generally written as:

$$\begin{aligned} C_{i/j}^{Y/\Gamma, [1]}(y, \kappa, \mathbf{b}; \mu, \zeta) &= R_{i/j}^{Y/\Gamma, [1]}(y, \kappa) - \delta_{Y\Gamma} \mathcal{P}_{i/j}^{\Gamma, [0]}(y, \kappa) \log \left(\frac{\mu^2 \mathbf{b}^2}{b_0^2} \right) \\ &- 2 \delta_{ij} \delta_{Y\Gamma} \delta(1-y) C_i \left[\frac{1}{2} \log^2 \left(\frac{\mu^2 \mathbf{b}^2}{b_0^2} \right) + \frac{\pi^2}{12} \right. \\ &\left. - \left(K_i + \log \left(\frac{\mu^2}{|1 - \kappa^2| \zeta} \right) - i s \pi \theta(\kappa - 1) \right) \log \left(\frac{\mu^2 \mathbf{b}^2}{b_0^2} \right) \right], \end{aligned} \quad (14)$$

where $b_0 = 2e^{-\gamma_E}$, with γ_E the Euler constant. The imaginary part in the third line and the $\log|1 - \kappa^2|$ emerges from the UV renormalization of the transverse momentum operator, we refer to App. A for the details. Here we limit ourselves to the following observation concerning the $\log|1 - \kappa^2|$. This logarithm diverges when $x = \xi$. Using as reference the pion-nucleon double Drell-Yan discussed in Ref. [50], this kinematic point is outside the factorisation region. Indeed, when $x = \xi$, one of the two partons from the nucleon carries vanishing longitudinal momentum, leading to $Q^2 \sim q_T^2$ for the virtual boson momentum, which contradicts the factorisation assumption of $Q^2 \gg q_T^2$. Therefore we conclude that, at least for the double Drell-Yan process, one cannot probe the region $x \sim \xi$ within the transverse-momentum factorisation.

Coming back to Eq. (14), the functions $\mathcal{P}_{i/j}^{\Gamma, [0]}$ are the one-loop GPD splitting functions (see Refs. [52–56]) and the constants K_i and C_i , for $i = q, g$ read:

$$\begin{aligned} K_q &= \frac{3}{2}, & C_q &= C_F, \\ K_g &= \frac{11}{6} - \frac{2n_f T_R}{3 C_A}, & C_g &= C_A. \end{aligned} \quad (15)$$

The one-loop *residual* functions $R_{i/j}^{Y/\Gamma, [1]}$ in Eq. (14) are computed here for the first time for the full set of leading-twist polarisations.⁴ These functions can be further decomposed as follows:

$$R_{i/j}^{Y/\Gamma, [1]}(y, \kappa) = \theta(1-y) \left[\theta(1+\kappa) r_{i/j}^{Y/\Gamma, [1]}(y, \kappa) + s_{Y/\Gamma} \theta(1-\kappa) r_{i/j}^{Y/\Gamma, [1]}(y, -\kappa) \right], \quad (16)$$

where $s_{Y/\Gamma} = -1$ when *either* Y or Γ is equal to L (so that $s_{L/L} = 1$), while $s_{Y/\Gamma} = 1$ otherwise. Results for all of the functions $r_{i/j}^{Y/\Gamma, [1]}(y, \kappa)$ are collected in Tab. 1, where rows correspond to GTMD parton species and polarisations (i, Y) , and columns to GPD parton species and polarisations (j, Γ) . As anticipated above, this table clearly shows that GTMD and GPD polarisations mix upon matching. For details on the computational methods used to obtain the functions in Tab. 1, we refer the reader to Refs. [30, 56, 57].

³This is standard practice in the case of forward distributions, where one trades quark distributions at negative values of x for the corresponding anti-quark distributions. Gluon distributions are instead either symmetric or anti-symmetric under $x \rightarrow -x$, depending on the polarisation.

⁴Ref. [30] presented results for $C_{i/j}^{U/U, [1]}$ only.

i, Y	j, Γ	q, U	g, U	q, L	g, L	q, T	g, T
q, U		$C_F \frac{1+\kappa}{\kappa(1+\kappa y)}$	$\frac{y(\kappa+1)}{\kappa(1+\kappa y)^2(1-\kappa y+i\delta)}$	0	0	0	$\frac{y(1+\kappa)}{\kappa(1+\kappa y)^2(1-\kappa y+i\delta)}$
g, U		$-C_F \frac{1-\kappa^2}{\kappa(1+\kappa y)}$	$C_A \left[\frac{2(1+\kappa)}{(1+\kappa y)^2} - \frac{\kappa(1+\kappa y)(1-\kappa y+i\delta)}{\kappa(1+\kappa y)^2(1-\kappa y+i\delta)} \right]$	0	0	0	$-C_A \frac{2y(1+\kappa)}{\kappa(1+\kappa y)^2(1-\kappa y+i\delta)}$
q, L		0	0	$C_F \frac{1+\kappa}{\kappa(1+\kappa y)}$	$1+\kappa$	0	$\frac{y(1+\kappa)}{\kappa(1+\kappa y)^2(1-\kappa y+i\delta)}$
g, L		0	0	$\frac{2(\kappa+1)C_F}{\kappa(1+\kappa y)}$	$\frac{\kappa(1+\kappa y)^2(1-\kappa y+i\delta)}{4(1+\kappa)}$	0	$\frac{(1+\kappa y)^2(1-\kappa y+i\delta)}{4y(1+\kappa)}$
q, T		0	0	0	0	0	0
g, T		$-C_F \frac{2(1+\kappa)}{\kappa y(1+\kappa y)}$	$-C_A \frac{2(1+\kappa)(1+\kappa^2 y^2)}{\kappa y(1+\kappa y)^2(1-\kappa y+i\delta)}$	$\frac{2(\kappa+1)C_F}{1+\kappa y}$	$\frac{4(\kappa+1)C_A}{(1+\kappa y)^2(1-\kappa y+i\delta)}$	0	$-C_A \frac{4\kappa y(1+\kappa)}{(1+\kappa y)^2(1-\kappa y+i\delta)}$

Table 1: Results for $r_{i/j}^{Y/\Gamma}(y, \kappa)$. Rows correspond to the GTMD parton species and polarisation (i, Y), while columns to the GPD parton species and polarisation (j, Γ). The presence of the term $i\delta$ appearing in some denominators is discussed in App. A.

Given the decomposition in Eq. (16), it is convenient to construct specific combinations of GTMDs that are more suited for a numerical implementation of the matching. We define the flavour non-singlet GTMD combination as:

$$\mathcal{F}^{[Y],-} = \sum_{q=1}^{n_f} \mathcal{F}_{q \leftarrow H}^{[Y]} - \mathcal{F}_{\bar{q} \leftarrow H}^{[Y]}, \quad (17)$$

and the flavour singlet GTMD combination as:

$$\mathcal{F}^{[Y],+} = \begin{pmatrix} \sum_{q=1}^{n_f} \mathcal{F}_{q \leftarrow H}^{[Y]} + \mathcal{F}_{\bar{q} \leftarrow H}^{[Y]} \\ \mathcal{F}_{g \leftarrow H}^{[Y]} \end{pmatrix}, \quad (18)$$

where the index q runs over the n_f active quark flavors. Using these combinations, the non-singlet residual function $R^{Y/\Gamma,-,[1]}$ acting on the combination $\mathcal{F}^{[Y],-}$ takes the form:

$$R^{Y/\Gamma,-,[1]}(y, \kappa) = \theta(1-y)R_1^{Y/\Gamma,-,[1]}(y, \kappa) + \theta(\kappa-1)R_2^{Y/\Gamma,-,[1]}(y, \kappa), \quad (19)$$

where:

$$\begin{aligned} R_1^{Y/\Gamma,-,[1]}(y, \kappa) &= r_{q/q}^{Y/\Gamma}(y, \kappa) + r_{q/q}^{Y/\Gamma}(y, -\kappa), \\ R_2^{Y/\Gamma,-,[1]}(y, \kappa) &= -r_{q/q}^{Y/\Gamma}(y, -\kappa) + s_\Gamma r_{q/q}^{Y/\Gamma}(-y, -\kappa), \end{aligned} \quad (20)$$

with $s_\Gamma = 1$ for $\Gamma = U, T$ and $s_\Gamma = -1$ for $\Gamma = L$. The singlet residual function $R^{Y/\Gamma,+,[1]}$ acting on the combination $\mathcal{F}^{[Y],+}$ is instead a 2×2 matrix in flavour space and its components can be written as:

$$\begin{aligned} R_{i/j}^{Y/\Gamma,+,[1]}(y, \kappa) &= \theta(1-y)\theta(1-\kappa)R_{1,i/j}^{Y/\Gamma,+,[1]}(y, \kappa) + \theta(y-1)\theta(\kappa-1)R_{2,i/j}^{Y/\Gamma,+,[1]}(y, \kappa) \\ &+ \theta(1-y)\theta(\kappa-1) \left(\widehat{R}_{i/j}^{Y/\Gamma,+,[1]}(y, \kappa) + \Sigma_{i/j}^{Y/\Gamma,+,[1]}(\kappa) \left[\text{PV} \left(\frac{1}{1-\kappa y} \right) - \frac{i\pi s}{\kappa} \delta \left(y - \frac{1}{\kappa} \right) \right] \right), \end{aligned} \quad (21)$$

where PV indicates the principal-value prescription and, as above, $s = \pm 1$ is the light-cone direction of the Wilson line. The functions $R_{1,i/j}^{Y/\Gamma,+,[1]}$ and $R_{2,i/j}^{Y/\Gamma,+,[1]}$ are defined as:

$$\begin{aligned} R_{1,i/j}^{Y/\Gamma,+,[1]}(y, \kappa) &= r_{i/j}^{Y/\Gamma}(y, \kappa) + s_{Y/\Gamma} r_{i/j}^{Y/\Gamma}(y, -\kappa), \\ R_{2,i/j}^{Y/\Gamma,+,[1]}(y, \kappa) &= -s_{Y/\Gamma} r_{i/j}^{Y/\Gamma}(y, -\kappa) - s_\Gamma r_{i/j}^{Y/\Gamma}(-y, -\kappa), \end{aligned} \quad (22)$$

while the functions $\widehat{R}_{i/j}^{Y/\Gamma,+,[1]}$ and the coefficients $\Sigma_{i/j}^{Y/\Gamma,+,[1]}$ derive from the equality:

$$R_{1,i/j}^{Y/\Gamma,+,[1]}(y, \kappa) + R_{2,i/j}^{Y/\Gamma,+,[1]}(y, \kappa) = \widehat{R}_{i/j}^{Y/\Gamma,+,[1]}(y, \kappa) + \frac{\Sigma_{i/j}^{Y/\Gamma,+,[1]}(\kappa)}{1-\kappa y + i s \delta}. \quad (23)$$

This equality is meant to isolate the singularity at $y = 1/\kappa$ exhibited by the combination $R_{1,i/j}^{Y/\Gamma,+,[1]} + R_{2,i/j}^{Y/\Gamma,+,[1]}$ in the term proportional to $\Sigma_{i/j}^{Y/\Gamma,+,[1]}$, while the term $\widehat{R}_{i/j}^{Y/\Gamma,+,[1]}$ is regular at this point. We point out that Eq. (21) is engineered to avoid overlapping regions between different terms in a way to make explicit the absence of non-integrable singularities. We refer the reader to App. A for more details on the origin of the imaginary part in the second line of Eq. (21). In view of an implementation, a numerically amenable formulation of PV prescription, when convoluted with a regular function f , is achieved as follows:

$$\int_x^\infty dy \theta(1-y) \text{PV} \left(\frac{1}{1-\kappa y} \right) f(y) = \quad (24)$$

$$\int_x^1 \frac{dy}{1-\kappa y} \left[f(y) - f\left(\frac{1}{\kappa}\right) \left(1 + \theta(\kappa y - 1) \frac{1-\kappa y}{\kappa y} \right) \right] + f\left(\frac{1}{\kappa}\right) \frac{1}{\kappa} \log \left(\frac{\kappa(1-\kappa x)}{\kappa-1} \right).$$

We finally give explicit expressions for the terms involved in the r.h.s. of Eqs. (19) and (21). As evident from Tab. 1, in the non-singlet case, Eq. (19), there are only two polarisation channels that get a q/q contribution necessary to construct $R_1^{Y/\Gamma,-,[1]}$ and $R_2^{Y/\Gamma,-,[1]}$: U/U and L/L . Using Eq. (20), the corresponding expressions read:

$$\begin{cases} R_1^{U/U,-,[1]}(y, \kappa) = C_F \frac{2(1-y)}{1-\kappa^2 y^2}, & R_1^{L/L,-,[1]}(y, \kappa) = C_F \frac{2(1-y)}{1-\kappa^2 y^2}, \\ R_2^{U/U,-,[1]}(y, \kappa) = C_F \frac{2y(1-\kappa)C_F}{1-\kappa^2 y^2}, & R_2^{L/L,-,[1]}(y, \kappa) = C_F \frac{2(1-\kappa)}{\kappa(1-\kappa^2 y^2)}. \end{cases} \quad (25)$$

In the singlet case, Eq. (21), explicit expressions for $R_{1,i/j}^{Y/\Gamma,+,[1]}$, $R_{2,i/j}^{Y/\Gamma,+,[1]}$, $\widehat{R}_{i/j}^{Y/\Gamma,+,[1]}$, and $\Sigma_{i/j}^{Y/\Gamma,+,[1]}$, obtained by means of Eqs. (22) and (23), are collected in Tabs. 2, 3, 4, and 5, respectively.

$i, Y \backslash j, \Gamma$	q, U	g, U	q, L	g, L	q, T	g, T
q, U	$C_F \frac{2(1-y)}{1-\kappa^2 y^2}$	$n_f \frac{4y(1-y)}{(1-\kappa^2 y^2)^2}$	0	0	0	$n_f \frac{4y(1-y)}{(1-\kappa^2 y^2)^2}$
g, U	$C_F \frac{2y(1-\kappa^2)}{1-\kappa^2 y^2}$	$-C_A \frac{8\kappa^2 y(1-y)}{(1-\kappa^2 y^2)^2}$	0	0	0	$-C_A \frac{4(1+\kappa^2)y(1-y)}{(1-\kappa^2 y^2)^2}$
q, L	0	0	$C_F \frac{2(1-y)}{1-\kappa^2 y^2}$	$n_f \frac{4(1-y)}{(1-\kappa^2 y^2)^2}$	0	$n_f \frac{4\kappa y(1-y)}{(1-\kappa^2 y^2)^2}$
g, L	0	0	$-C_F \frac{4(1-y)}{1-\kappa^2 y^2}$	$-C_A \frac{8(1-y)}{(1-\kappa^2 y^2)^2}$	0	$-C_A \frac{8\kappa y(1-y)}{(1-\kappa^2 y^2)^2}$
q, T	0	0	0	0	0	0
g, T	$-C_F \frac{4(1-y)}{y(1-\kappa^2 y^2)}$	$-C_A \frac{4(1-y)(1+\kappa^2 y^2)}{y(1-\kappa^2 y^2)^2}$	$C_F \frac{4\kappa(1-y)}{1-\kappa^2 y^2}$	$C_A \frac{8\kappa(1-y)}{(1-\kappa^2 y^2)^2}$	0	$-C_A \frac{8\kappa^2 y(1-y)}{(1-\kappa^2 y^2)^2}$

Table 2: Results for the functions $R_{1,i/j}^{Y/\Gamma,+,[1]}$ in the r.h.s. of Eq. (21). Rows correspond to the GTMD parton species and polarisation (i, Y), while columns to the GPD parton species and polarisation (j, Γ).

$i, Y \backslash j, \Gamma$	q, U	g, U	q, L	g, L	q, T	g, T
q, U	$C_F \frac{2(1-\kappa)}{\kappa(1-\kappa^2 y^2)}$	$n_f \frac{4y^2(1-\kappa)}{(1-\kappa^2 y^2)^2}$	0	0	0	$n_f \frac{4y^2(1-\kappa)}{(1-\kappa^2 y^2)^2}$
g, U	$-C_F \frac{2(1-\kappa^2)}{\kappa(1-\kappa^2 y^2)}$	$-2C_A \frac{1-\kappa}{1-\kappa^2 y^2} \left[\frac{1-\kappa}{\kappa} + \frac{2(1+\kappa^2 y^2)}{1-\kappa^2 y^2} \right]$	0	0	0	$-C_A \frac{4y^2(1-\kappa)(1+\kappa^2)}{(1-\kappa^2 y^2)^2}$
q, L	0	0	$C_F \frac{2y(1-\kappa)}{1-\kappa^2 y^2}$	$n_f \frac{4y(1-\kappa)}{(1-\kappa^2 y^2)^2}$	0	$n_f \frac{4y(1-\kappa)}{(1-\kappa^2 y^2)^2}$
g, L	0	0	$-C_F \frac{4y(1-\kappa)}{1-\kappa^2 y^2}$	$-C_A \frac{8y(1-\kappa)}{(1-\kappa^2 y^2)^2}$	0	$-C_A \frac{8y(1-\kappa)}{(1-\kappa^2 y^2)^2}$
q, T	0	0	0	0	0	0
g, T	$-C_F \frac{4(1-\kappa)}{1-\kappa^2 y^2}$	$-C_A \frac{4(1-\kappa)(1+\kappa^2 y^2)}{(1-\kappa^2 y^2)^2}$	$C_F \frac{4(1-\kappa)}{1-\kappa^2 y^2}$	$C_A \frac{8(1-\kappa)}{(1-\kappa^2 y^2)^2}$	0	$-C_A \frac{8\kappa^2 y^2(1-\kappa)}{(1-\kappa^2 y^2)^2}$

Table 3: Same as Tab. 2 but for $R_{2,i/j}^{Y/\Gamma,+,[1]}$.

We conclude this section by discussing the forward limit of the matching functions, which amounts to taking the limit $\kappa \rightarrow 0$. Given the decompositions in Eqs. (19) and (21), we only need to consider the limit of the functions $R_1^{Y/\Gamma,-,[1]}$ and $R_{1,i/j}^{Y/\Gamma,+,[1]}$. Moreover, since $R_1^{Y/\Gamma,-,[1]}(y, 0) = R_{1,q/q}^{Y/\Gamma,+,[1]}(y, 0)$, it is enough to consider the forward limit of the latter set of functions, which is collected in Tab. 6. We first notice that the known results for the TMD matching functions are consistently recovered (see, *e.g.*, Ref. [16, 58]). We also point out that in Tab. 6 we removed the rightmost column corresponding to the linearly-polarised gluon PDF (*i.e.* the forward limit of the linearly-polarised gluon GPD). The reason is that this distribution can only exist in hadrons with spin equal to or larger than one [59, 60]. Since here we are only concerned with the

$i, Y \backslash j, \Gamma$	q, U	g, U	q, L	g, L	q, T	g, T
q, U	$C_F \frac{2}{\kappa(1+\kappa y)}$	$-n_f \frac{1-\kappa y}{\kappa(1+\kappa y)^2}$	0	0	0	$-n_f \frac{1-\kappa y}{\kappa(1+\kappa y)^2}$
g, U	$-C_F \frac{2(1-\kappa^2)}{\kappa(1+\kappa y)}$	$C_A \frac{1}{1+\kappa y} \left[\frac{4\kappa}{1+\kappa y} - \frac{1+\kappa^2}{\kappa} \right]$	0	0	0	$C_A \frac{(1+\kappa^2)(1-\kappa y)}{\kappa(1+\kappa y)^2}$
q, L	0	0	$\frac{2C_F}{1+\kappa y}$	$n_f \frac{3+\kappa y}{(1+\kappa y)^2}$	0	$-n_f \frac{1-\kappa y}{\kappa(1+\kappa y)^2}$
g, L	0	0	$-\frac{4C_F}{1+\kappa y}$	$-C_A \frac{2(3+\kappa y)}{(1+\kappa y)^2}$	0	$C_A \frac{2(1-\kappa y)}{\kappa(1+\kappa y)^2}$
q, T	0	0	0	0	0	0
g, T	$-C_F \frac{4}{y(1+\kappa y)}$	$C_A \left[\frac{2\kappa}{1+\kappa y} + \frac{4\kappa}{(1+\kappa y)^2} - \frac{4}{y} \right]$	$\frac{4C_F}{1+\kappa y}$	$C_A \frac{2(3+\kappa y)}{(1+\kappa y)^2}$	0	$C_A \frac{2\kappa(1-\kappa y)}{(1+\kappa y)^2}$

Table 4: Same as Tab. 2 but for $\widehat{R}_{i/j}^{Y/\Gamma,+, [1]}$.

$i, Y \backslash j, \Gamma$	q, U	g, U	q, L	g, L	q, T	g, T
q, U	0	$\frac{n_f}{\kappa}$	0	0	0	$\frac{n_f}{\kappa}$
g, U	0	$-\frac{(1+\kappa^2)C_A}{\kappa}$	0	0	0	$-\frac{(1+\kappa^2)C_A}{\kappa}$
q, L	0	0	0	n_f	0	$\frac{n_f}{\kappa}$
g, L	0	0	0	$-2C_A$	0	$-\frac{2C_A}{\kappa}$
q, T	0	0	0	0	0	0
g, T	0	$-2\kappa C_A$	0	$2C_A$	0	$-2\kappa C_A$

Table 5: Same as Tab. 2 but for $\Sigma_{i/j}^{Y/\Gamma,+, [1]}$.

proton (see below), we can neglect this distribution. Therefore, even those matching functions associated with the linearly-polarised gluon PDFs which survive the forward limit, such as $R_{1,q/g}^{U/T,+, [1]}$ and $R_{1,g/g}^{U/T,+, [1]}$, would give a vanishing contribution to the corresponding TMD.

$i, Y \backslash j, \Gamma$	q, U	g, U	q, L	g, L	q, T
q, U	$2C_F(1-y)$	$4n_f y(1-y)$	0	0	0
g, U	$2C_F y$	0	0	0	0
q, L	0	0	$2C_F(1-y)$	$4n_f(1-y)$	0
g, L	0	0	$-4C_F(1-y)$	$-8C_A(1-y)$	0
q, T	0	0	0	0	0
g, T	$-4C_F \frac{1-y}{y}$	$-4C_A \frac{1-y}{y}$	0	0	0

Table 6: Forward limit (i.e. $\kappa \rightarrow 0$) of the functions $R_{1,i/j}^{Y/\Gamma,+, [1]}$ given in Tab. 2.

4 Matching for specific parametrisations

In the previous section, we obtained the matching functions for GTMDs on GPDs by considering the appropriate matrix elements (Eqs. (3) and (4) for GTMDs, and Eqs. (5) and (6) for

GPDs). Restricting to the case of a proton target ($H = p$), we now need to adopt specific parametrisations for both GTMD and GPD correlators and establish their matching at the level of single distributions. To this purpose, we use a modified version of the GTMD parametrisation presented in Ref. [33], which in turn slightly differs from that of Ref. [32]. In the following, we quickly review the logic behind its construction. The easiest way to derive the matching relations between GTMDs and GPDs is to use the helicity basis for the proton state in which the matrix elements in Eqs. (3) and (4) can generally be written as:

$$\mathcal{F}_{i/H}^{[Y]}(x, \xi, \mathbf{b}, \Delta_T) = \bar{u}_{\lambda'}(p') \frac{M_i^Y(x, \xi, \mathbf{b}, \Delta_T)}{2p^+(1-\xi^2)} u_{\lambda}(p), \quad (26)$$

with u and \bar{u} being the spinors of incoming and outgoing protons, respectively. Dropping all arguments, the decompositions for polarisations U and L is the same for quarks and gluons and read:

$$M_i^U = \gamma^+ \left(S_{1,1a}^{0;+;i} + \gamma_5 \frac{i\varepsilon_T^{b\Delta_T}}{M|\mathbf{b}|} S_{1,1b}^{0;+;i} \right) - i\sigma^{\mu+} \left(\frac{b_{\mu}}{|\mathbf{b}|} P_{1,1a}^{0;+;i} + \frac{\Delta_{T,\mu}}{M} P_{1,1b}^{0;+;i} \right), \quad (27)$$

$$M_i^L = \gamma^+ \gamma_5 \left(S_{1,1a}^{0;-;i} + \gamma_5 \frac{i\varepsilon_T^{b\Delta_T}}{M|\mathbf{b}|} S_{1,1b}^{0;-;i} \right) - i\sigma^{\mu+} \gamma_5 \left(\frac{b_{\mu}}{|\mathbf{b}|} P_{1,1a}^{0;-;i} + \frac{\Delta_{T,\mu}}{M} P_{1,1b}^{0;-;i} \right), \quad (28)$$

with $i = q, g$ and where M is the proton mass. For polarisation T , quark and gluon decompositions are different and read:

$$M_q^T = \sqrt{2} i\varepsilon_T^{R\mu} \gamma^+ \left(b_{\mu} M P_{1,1a}^{1;-;q} + \frac{\Delta_{T,\mu}}{M} P_{1,1b}^{1;-;q} \right) + \sqrt{2} \gamma^+ \gamma_5 \left(b_R M P_{1,1a}'^{1;-;q} + \frac{\Delta_R}{M} P_{1,1b}'^{1;-;q} \right) + \frac{\sqrt{2} i\sigma^{R+} \gamma_5}{2} \left(S_{1,1a}^{1;-;q} - \gamma_5 i\varepsilon_T^{b\Delta_T} S_{1,1b}^{1;-;q} \right) + \sqrt{2} i\sigma^{L+} \gamma_5 \left(\frac{b_R^2}{\mathbf{b}^2} D_{1,1a}^{1;-;q} + \frac{\Delta_R^2}{M^2} D_{1,1b}^{1;-;q} \right), \quad (29)$$

$$M_g^T = 2\gamma^+ \left(\frac{b_R^2}{\mathbf{b}^2} D_{1,1a}^{2;+;g} + \frac{\Delta_R^2}{M^2} D_{1,1b}^{2;+;g} \right) - 2i\varepsilon_T^{R\mu} \gamma^+ \gamma_5 \left(\frac{b_{\mu} b_R}{\mathbf{b}^2} D_{1,1a}'^{2;+;g} + \frac{\Delta_{T,\mu} \Delta_R}{M^2} D_{1,1b}'^{2;+;g} \right) - i\sigma^{R+} \left(\frac{b_R}{|\mathbf{b}|} P_{1,1a}^{2;+;g} + \frac{\Delta_R}{M} P_{1,1b}^{2;+;g} \right) + 2i\sigma^{L+} \left(\frac{b_R \Delta_R}{M \mathbf{b}^2} F_{1,1a}'^{2;+;g} + \frac{b_R \Delta_R^2}{M^2 |\mathbf{b}|} F_{1,1b}'^{2;+;g} \right). \quad (30)$$

As mentioned above, this is a modified version of the parametrisation of Ref. [33] in different respects. First, Ref. [33] provides expressions in momentum space. This is inconvenient for matching, which takes place naturally in position space. We thus do the replacement $k_T^{\mu}/M \rightarrow b^{\mu}/|\mathbf{b}|$, but keeping the same structures. Second, we replace the factor $\sqrt{1-\xi^2}$ in Eq. (3.52) of Ref. [33] with $(1-\xi^2)$, see Eq. (26). The net result is that $\mathcal{F}_{\text{here}} = \mathcal{F}_{[33]}/\sqrt{1-\xi^2}$. This allows us to get rid of an overall factor of $\sqrt{1-\xi^2}$ in the matching functions. Finally, the distributions $F_{1,1a}'^{2;+;g}$ and $F_{1,1b}'^{2;+;g}$ appearing in the decomposition of M_g^T could in principle be written as the following combinations of the distributions $F_{1,1a}^{2;+;g}$ and $F_{1,1b}^{2;+;g}$ of Ref. [33]:

$$F_{1,1a}'^{2;+;g} = \frac{1}{\sqrt{1-\xi^2}} \left[\frac{2M^2(\mathbf{b} \cdot \Delta_T)}{\Delta_T^2} F_{1,1a}^{2;+;g} - \frac{\Delta_T^2}{M^2} F_{1,1b}^{2;+;g} \right], \quad (31)$$

$$F_{1,1b}'^{2;+;g} = \frac{1}{\sqrt{1-\xi^2}} \left[\frac{2(\mathbf{b} \cdot \Delta_T)}{M|\mathbf{b}|} F_{1,1b}^{2;+;g} - \frac{M^3|\mathbf{b}|}{\Delta_T^2} F_{1,1a}^{2;+;g} \right]. \quad (32)$$

However, the tensor structures in front of the non-primed distributions do not naturally emerge from the matching, leading to needlessly complex expressions. In what follows, we will thus only consider $F_{1,1a}^{2;+;g}$ and $F_{1,1b}^{2;+;g}$, rather than their non-primed counterparts.

As far as GPDs are concerned, we use the standard parametrisation of Ref. [32], where the leading-twist quark and gluon distributions $H^i, E^i, \tilde{H}^i, \tilde{E}^i, H_T^i, E_T^i, \tilde{H}_T^i, \tilde{E}_T^i$, with $i = q, g$, are defined.

We are now in a position to give the matching of GTMDs on GPDs for each individual distribution. Unpolarised quark GTMD distributions read:

$$S_{1,1a}^{0;+;q} = c_{q/q}^{U/U} \otimes [(1 - \xi^2)H^q - \xi^2 E^q] + c_{q/g}^{U/U} \otimes [(1 - \xi^2)H^g - \xi^2 E^g] \quad (33)$$

$$- \frac{2(\mathbf{b} \cdot \Delta_T)^2 - \mathbf{b}^2 \Delta_T^2}{4M^2 \mathbf{b}^2} c_{q/g}^{U/T} \otimes [E_T^g - \xi \tilde{E}_T^g + 2\tilde{H}_T^g],$$

$$S_{1,1b}^{0;+;q} = \frac{(\mathbf{b} \cdot \Delta_T)}{2M|\mathbf{b}|} c_{q/g}^{U/T} \otimes [\xi E_T^g - \tilde{E}_T^g], \quad (34)$$

$$P_{1,1a}^{0;+;q} = \frac{(\mathbf{b} \cdot \Delta_T)}{M|\mathbf{b}|} c_{q/g}^{U/T} \otimes [(1 - \xi^2)H_T^g + \xi \tilde{E}_T^g - \xi^2 E_T^g], \quad (35)$$

$$P_{1,1b}^{0;+;q} = \frac{1}{2} \left(c_{q/q}^{U/U} \otimes E^q + c_{q/g}^{U/U} \otimes E^g \right) \quad (36)$$

$$- \frac{1}{2} c_{q/g}^{U/T} \otimes \left[(1 - \xi^2)H_T^g + \xi \tilde{E}_T^g - \xi^2 E_T^g - \frac{2(\mathbf{b} \cdot \Delta_T)^2 - \mathbf{b}^2 \Delta_T^2}{2M^2 \mathbf{b}^2} \tilde{H}_T^g \right].$$

Longitudinally-polarised quark GTMDs read:

$$S_{1,1a}^{0;-;q} = c_{q/q}^{L/L} \otimes [(1 - \xi^2)\tilde{H}^q - \xi^2 \tilde{E}^q] + c_{q/g}^{L/L} \otimes [(1 - \xi^2)\tilde{H}^g - \xi^2 \tilde{E}^g] \quad (37)$$

$$+ \frac{2(\mathbf{b} \cdot \Delta_T)^2 - \mathbf{b}^2 \Delta_T^2}{4M^2 \mathbf{b}^2} c_{q/g}^{L/T} \otimes [\tilde{E}_T^g - \xi E_T^g],$$

$$S_{1,1b}^{0;-;q} = \frac{(\mathbf{b} \cdot \Delta_T)}{2M|\mathbf{b}|} c_{q/g}^{L/T} \otimes [E_T^g - \xi \tilde{E}_T^g + 2\tilde{H}_T^g], \quad (38)$$

$$P_{1,1a}^{0;-;q} = \frac{(\mathbf{b} \cdot \Delta_T)}{M|\mathbf{b}|} c_{q/g}^{L/T} \otimes \left[(1 - \xi^2)H_T^g + \xi \tilde{E}_T^g - \xi^2 E_T^g + \frac{\Delta_T^2}{2M^2} \tilde{H}_T^g \right], \quad (39)$$

$$P_{1,1b}^{0;-;q} = \frac{1}{2} \left(c_{q/q}^{L/L} \otimes [\xi \tilde{E}^q] + c_{q/g}^{L/L} \otimes [\xi \tilde{E}^g] \right) \quad (40)$$

$$- \frac{1}{2} c_{q/g}^{L/T} \otimes \left[(1 - \xi^2)H_T^g + \xi \tilde{E}_T^g - \xi^2 E_T^g + \frac{(\mathbf{b} \cdot \Delta_T)^2}{M^2 \mathbf{b}^2} \tilde{H}_T^g \right].$$

Transversely-polarised quark GTMDs read:

$$S_{1,1a}^{1;-;q} = 2c_{q/q}^{T/T} \otimes \left[(1 - \xi^2)H_T^q + \xi \tilde{E}_T^q - \xi^2 E_T^q + \frac{\Delta_T^2}{4M^2} \tilde{H}_T^q \right], \quad (41)$$

$$P_{1,1b}^{1;-;q} = \frac{1}{2} c_{q/q}^{T/T} \otimes [E_T^q - \xi \tilde{E}_T^q + 2\tilde{H}_T^q], \quad (42)$$

$$P'_{1,1b}{}^{1;-;q} = \frac{1}{2} c_{q/q}^{T/T} \otimes [\tilde{E}_T^q - \xi E_T^q], \quad (43)$$

$$D_{1,1b}^{1;-;q} = -\frac{1}{2} c_{q/q}^{T/T} \otimes \tilde{H}_T^q. \quad (44)$$

For unpolarised and longitudinally-polarised gluon GTMDs, the structure of the matching is analogous to that of quarks. Specifically, for unpolarised gluons GTMDs we have:

$$S_{1,1a}^{0;+;g} = c_{g/g}^{U/U} \otimes [(1 - \xi^2)H^g - \xi^2 E^g] + c_{g/q}^{U/U} \otimes [(1 - \xi^2)H^q - \xi^2 E^q] \quad (45)$$

$$- \frac{2(\mathbf{b} \cdot \Delta_T)^2 - \mathbf{b}^2 \Delta_T^2}{4M^2 \mathbf{b}^2} c_{g/g}^{U/T} \otimes [E_T^g - \xi \tilde{E}_T^g + 2\tilde{H}_T^g],$$

$$S_{1,1b}^{0;+;g} = \frac{(\mathbf{b} \cdot \Delta_T)}{2M|\mathbf{b}|} c_{g/g}^{U/T} \otimes [\xi E_T^g - \tilde{E}_T^g], \quad (46)$$

$$P_{1,1a}^{0;+;g} = \frac{(\mathbf{b} \cdot \Delta_T)}{M|\mathbf{b}|} c_{g/g}^{U/T} \otimes [(1 - \xi^2)H_T^g + \xi \tilde{E}_T^g - \xi^2 E_T^g], \quad (47)$$

$$P_{1,1b}^{0;+;g} = \frac{1}{2} \left(c_{g/g}^{U/U} \otimes E^g + c_{g/q}^{U/U} \otimes E^q \right) \quad (48)$$

$$- \frac{1}{2} c_{g/g}^{U/T} \otimes \left[(1 - \xi^2)H_T^g + \xi \tilde{E}_T^g - \xi^2 E_T^g - \frac{2(\mathbf{b} \cdot \Delta_T)^2 - \mathbf{b}^2 \Delta_T^2}{2M^2 \mathbf{b}^2} \tilde{H}_T^g \right],$$

and for longitudinally-polarised gluon GTMDs, we have:

$$S_{1,1a}^{0;-;g} = c_{g/g}^{L/L} \otimes \left[(1 - \xi^2) \tilde{H}^g - \xi^2 \tilde{E}^g \right] + c_{g/q}^{L/L} \otimes \left[(1 - \xi^2) \tilde{H}^q - \xi^2 \tilde{E}^q \right] \\ + \frac{2(\mathbf{b} \cdot \boldsymbol{\Delta}_T)^2 - \mathbf{b}^2 \Delta_T^2}{4M^2 \mathbf{b}^2} c_{g/g}^{L/T} \otimes \left[\tilde{E}_T^g - \xi E_T^g \right], \quad (49)$$

$$S_{1,1b}^{0;-;g} = \frac{(\mathbf{b} \cdot \boldsymbol{\Delta}_T)}{2M|\mathbf{b}|} c_{g/g}^{L/T} \otimes \left[E_T^g - \xi \tilde{E}_T^g + 2\tilde{H}_T^g \right], \quad (50)$$

$$P_{1,1a}^{0;-;g} = \frac{(\mathbf{b} \cdot \boldsymbol{\Delta}_T)}{M|\mathbf{b}|} c_{g/g}^{L/T} \otimes \left[(1 - \xi^2) H_T^g + \xi \tilde{E}_T^g - \xi^2 E_T^g + \frac{\Delta_T^2}{2M^2} \tilde{H}_T^g \right], \quad (51)$$

$$P_{1,1b}^{0;-;g} = \frac{1}{2} \left(c_{g/g}^{L/L} \otimes [\xi \tilde{E}^g] + c_{g/q}^{L/L} \otimes [\xi \tilde{E}^q] \right) \\ - \frac{1}{2} c_{g/g}^{L/T} \otimes \left[(1 - \xi^2) H_T^g + \xi \tilde{E}_T^g - \xi^2 E_T^g + \frac{(\mathbf{b} \cdot \boldsymbol{\Delta}_T)^2}{M^2 \mathbf{b}^2} \tilde{H}_T^g \right]. \quad (52)$$

For the linearly-polarised gluons GTMDs, the parametrisation differs from that of quarks and the picture is more complicated. In particular, there are eight distributions that match onto GPDs and they are given by:

$$P_{1,1a}^{2;+;g} = -\frac{(\mathbf{b} \cdot \boldsymbol{\Delta}_T)}{M|\mathbf{b}|} \left(c_{g/g}^{T/U} \otimes E^g - c_{g/g}^{T/L} \otimes [\xi \tilde{E}^g] + c_{g/q}^{T/U} \otimes E^q - c_{g/q}^{T/L} \otimes [\xi \tilde{E}^q] \right), \quad (53)$$

$$P_{1,1b}^{2;+;g} = -c_{g/g}^{T/T} \otimes \left[(1 - \xi^2) H_T^g + \xi \tilde{E}_T^g - \xi^2 E_T^g + \frac{\Delta_T^2}{4M^2} \tilde{H}_T^g \right] \\ + \frac{1}{2} c_{g/g}^{T/U} \otimes E^g - \frac{1}{2} c_{g/g}^{T/L} \otimes [\xi \tilde{E}^g] + \frac{1}{2} c_{g/q}^{T/U} \otimes E^q - \frac{1}{2} c_{g/q}^{T/L} \otimes [\xi \tilde{E}^q], \quad (54)$$

$$D_{1,1a}^{2;+;g} = c_{g/q}^{T/U} \otimes \left[(1 - \xi^2) H^q - \xi^2 E^q \right] + c_{g/g}^{T/U} \otimes \left[(1 - \xi^2) H^g - \xi^2 E^g \right], \quad (55)$$

$$D_{1,1b}^{2;+;g} = -\frac{1}{4} c_{g/g}^{T/T} \otimes \left[E_T^g - \xi \tilde{E}_T^g + 2\tilde{H}_T^g \right], \quad (56)$$

$$D_{1,1a}'^{2;+;g} = c_{g/q}^{T/L} \otimes \left[(1 - \xi^2) \tilde{H}^q - \xi^2 \tilde{E}^q \right] + c_{g/g}^{T/L} \otimes \left[(1 - \xi^2) \tilde{H}^g - \xi^2 \tilde{E}^g \right], \quad (57)$$

$$D_{1,1b}'^{2;+;g} = -\frac{1}{4} c_{g/g}^{T/T} \otimes \left[\tilde{E}_T^g - \xi E_T^g \right], \quad (58)$$

$$F_{1,1a}'^{2;+;g} = -\frac{\Delta_T^2}{4M^2} c_{g/g}^{T/T} \otimes \tilde{H}_T^g + \frac{1}{2} c_{g/g}^{T/U} \otimes E^g + \frac{1}{2} c_{g/g}^{T/L} \otimes [\xi \tilde{E}^g] \\ + \frac{1}{2} c_{g/q}^{T/U} \otimes E^q + \frac{1}{2} c_{g/q}^{T/L} \otimes [\xi \tilde{E}^q], \quad (59)$$

$$F_{1,1b}'^{2;+;g} = \frac{(\mathbf{b} \cdot \boldsymbol{\Delta}_T)}{2M|\mathbf{b}|} c_{g/g}^{T/T} \otimes \tilde{H}_T^g. \quad (60)$$

We remark that, thanks to the dependence on the scalar product $\mathbf{b} \cdot \boldsymbol{\Delta}_T$, we find several non-vanishing GTMDs upon matching on twist-two GPDs. This is a consequence of the non-forward nature of GTMDs, which provides a second transverse vector that can couple to \mathbf{b} to generate angular modulations already at leading twist.

5 Reconstructing GTMDs

Having established the matching pattern of leading-twist GTMDs on GPDs, we turn to their evolution. This will complete the picture and allow us to reconstruct the full kinematics dependence of GTMDs. To discuss evolution, it is convenient to denote with $\mathbb{F}_i^{[Y]}$ any quark ($i = q$) or gluon ($i = g$) GTMD from an explicit parametrisation of polarisation Y . The evolution

equations with respect to the rapidity scale ζ and the renormalisation scale μ read:

$$\begin{aligned} \frac{d \log \mathbb{F}_i^{[Y]}(x, \xi, \mathbf{b}, \Delta_T; \mu, \zeta)}{d \log \sqrt{\zeta}} &= K_i(\mathbf{b}, \mu_b) - \int_{\mu_b}^{\mu} \frac{d\mu'}{\mu'} \gamma_{K,i}(\alpha_s(\mu')), \\ \frac{d \log \mathbb{F}_i^{[Y]}(x, \xi, \mathbf{b}, \Delta_T; \mu, \zeta)}{d \log \mu} &= \gamma_{F,i}(\alpha_s(\mu)) - \frac{\gamma_{K,i}(\alpha_s(\mu))}{2} \left(\log \left(\frac{|1 - \kappa^2| \zeta}{\mu} \right) + i s \pi \theta(\kappa - 1) \right), \end{aligned} \quad (61)$$

with $\mu_b = b_0/|\mathbf{b}|$ and where the anomalous dimensions $K_i(\mathbf{b}, \mu_b)$, $\gamma_{F,i}$, and $\gamma_{K,i}$ are all perturbative quantities and coincide with their forward TMD counterparts. In fact, the main differences between GTMD and TMD are the presence in the evolution equation w.r.t. μ of the factor $|1 - \kappa^2|$ inside the logarithm that multiplies $\gamma_{K,i}$ and of the imaginary part, which, as we will see below, plays a crucial role.⁵

The evolution equations in Eq. (61) can be solved explicitly. Choosing $\mu_0 = \mu_b$ and $\zeta_0 = \mu_b^2$ as boundary-condition scales, which prevent the presence of potentially large logarithms, the evolution of GTMDs to the scales μ and ζ is multiplicative and can be written as:

$$\mathbb{F}_i^{[Y]}(x, \xi, \mathbf{b}, \Delta_T; \mu, \zeta) = \mathcal{R}_i [(\mu, \zeta) \leftarrow (\mu_b, \mu_b^2)] \mathbb{F}_i^{[Y]}(x, \xi, \mathbf{b}, \Delta_T; \mu_b, \mu_b^2), \quad (62)$$

where the factor \mathcal{R}_i , often referred to as Sudakov form factor, has the following form:

$$\begin{aligned} \mathcal{R}_i [(\mu, \zeta) \leftarrow (\mu_b, \mu_b^2)] &= \exp \left\{ \frac{1}{2} K_i(\mathbf{b}, \mu_b) \log \left(\frac{|1 - \kappa^2| \zeta}{\mu_b^2} \right) \right. \\ &+ \int_{\mu_b}^{\mu} \frac{d\mu'}{\mu'} \left[\gamma_{F,i}(\alpha_s(\mu')) - \frac{1}{2} \gamma_{K,i}(\alpha_s(\mu')) \log \left(\frac{|1 - \kappa^2| \zeta}{\mu'^2} \right) \right] \\ &\left. + \frac{i\pi s}{2} \theta(\kappa - 1) \left[K_i(\mathbf{b}, \mu_b) - \int_{\mu_b}^{\mu} \frac{d\mu'}{\mu'} \gamma_{K,i}(\alpha_s(\mu')) \right] \right\}. \end{aligned} \quad (63)$$

Factoring out the imaginary part of the argument of the exponential in Eq. (63) allows us to write:

$$\begin{aligned} \mathcal{R}_i [(\mu, \zeta) \leftarrow (\mu_b, \mu_b^2)] &= \\ &= R_i [(\mu, \zeta) \leftarrow (\mu_b, \mu_b^2)] \exp \left\{ s \frac{i\pi}{2} \theta(\kappa - 1) \left[K_i(\mathbf{b}, \mu_b) - \int_{\mu_b}^{\mu} \frac{d\mu'}{\mu'} \gamma_{K,i}(\alpha_s(\mu')) \right] \right\} \\ &= R_i [(\mu, \zeta) \leftarrow (\mu_b, \mu_b^2)] [\cos(\phi(\kappa, \mathbf{b}, \mu)) + i s \sin(\phi(\kappa, \mathbf{b}, \mu))], \end{aligned} \quad (64)$$

where R_i is real and we have defined the angle:

$$\phi(\kappa, \mathbf{b}, \mu) = \frac{\pi}{2} \theta(\kappa - 1) \left(K_i(\mathbf{b}, \mu_b) - \int_{\mu_b}^{\mu} \frac{d\mu'}{\mu'} \gamma_{K,i}(\alpha_s(\mu')) \right) = \frac{\pi}{2} \theta(\kappa - 1) K_i(\mathbf{b}, \mu), \quad (65)$$

where $K_i(\mathbf{b}, \mu)$, as opposed to $K_i(\mathbf{b}, \mu_b)$, is the *evolved* Collin-Soper kernel which governs the rapidity-scale evolution in Eq. (61).

Now, we use the fact that each GTMD can be decomposed into a T-even and a T-odd part as follows:

$$\mathbb{F}_i^{[Y]} = \mathbb{F}_i^{[Y],e} + i \mathbb{F}_i^{[Y],o}, \quad (66)$$

⁵As an aside note, we point out that a similar factor emerges in the evolution of twist-3 forward TMDs, see Ref. [28]. This happens because in both cases one has two independent longitudinal-momentum variables: for GTMDs, they are x and ξ , while for twist-3 TMDs they are any pair of longitudinal-momentum fractions of the three fields that define the operator. In both cases, the imaginary part in the evolution equations comes with the sign of the direction of the Wilson line s .

where $\mathbb{F}_i^{[Y],e}$ and $\mathbb{F}_i^{[Y],o}$ are both real functions. Moreover, $\mathbb{F}_i^{[Y],e}$ remains unchanged upon change of the direction of the Wilson line s , while $\mathbb{F}_i^{[Y],o}$ changes sign. Dropping all variables except the scales, Eq. (62) can be expressed in a matrix form for T-even and T-odd components as follows:

$$\begin{pmatrix} \mathbb{F}_i^{[Y],e}(\mu, \zeta) \\ \mathbb{F}_i^{[Y],o}(\mu, \zeta) \end{pmatrix} = R_i [(\mu, \zeta) \leftarrow (\mu_b, \mu_b^2)] \begin{pmatrix} \cos(\phi(\mu)) & -s \sin(\phi(\mu)) \\ s \sin(\phi(\mu)) & \cos(\phi(\mu)) \end{pmatrix} \begin{pmatrix} \mathbb{F}_i^{[Y],e}(\mu_b, \mu_b^2) \\ \mathbb{F}_i^{[Y],o}(\mu_b, \mu_b^2) \end{pmatrix}. \quad (67)$$

We note that the rotation matrix generated by the Sudakov form factor is diagonal in the DGLAP region ($\kappa < 1$) such that, as expected, T-even and T-odd GTMDs evolve independently in this region. Conversely, in the ERBL region ($\kappa > 1$), the rotation matrix does cause a mixing of the two distributions upon evolution.

The ‘‘initial-scale’’ GTMD $\mathbb{F}_i^{[Y]}(\mu_b, \mu_b^2)$ can now be obtained by means of matching on a suitable combination of collinear GPDs $f_j^{[\Gamma]}(\mu_b)$ through convolution with the appropriate matching functions, see Eq. (11):⁶

$$\mathbb{F}_i^{[Y]}(\mu_b, \mu_b^2) = \left[\mathcal{C}_{i/j}^{Y/\Gamma} \otimes f_j^{[\Gamma]} \right] (\mu_b, \mu_b^2). \quad (68)$$

Given a particular GTMD $\mathbb{F}_i^{[Y]}$, the appropriate set of GPDs $f_j^{[\Gamma]}$ that enter the r.h.s. of Eq. (68) can be read from Eqs. (33)-(60). As we have seen above, the matching functions $\mathcal{C}_{i/j}^{Y/\Gamma}$ also acquire an imaginary contribution (see Eq. (21)), so that one can write:⁷

$$\mathbb{F}_i^{[Y]}(\mu_b, \mu_b^2) = \left[\mathcal{C}_{i/j}^{Y/\Gamma,e} \otimes f_j^{[\Gamma]} \right] (\mu_b, \mu_b^2) + is \left[\mathcal{C}_{i/j}^{Y/\Gamma,o} \otimes f_j^{[\Gamma]} \right] (\mu_b, \mu_b^2), \quad (69)$$

which in matrix form reads:

$$\begin{pmatrix} \mathbb{F}_i^{[Y],e}(\mu_b, \mu_b^2) \\ \mathbb{F}_i^{[Y],o}(\mu_b, \mu_b^2) \end{pmatrix} = \left[\begin{pmatrix} \mathcal{C}_{i/j}^{Y/\Gamma,e} \\ s \mathcal{C}_{i/j}^{Y/\Gamma,o} \end{pmatrix} \otimes f_j^{[\Gamma]} \right] (\mu_b, \mu_b^2). \quad (70)$$

This equality can finally be used into Eq. (67), producing the result:

$$\begin{pmatrix} \mathbb{F}_i^{[Y],e}(\mu, \zeta) \\ \mathbb{F}_i^{[Y],o}(\mu, \zeta) \end{pmatrix} = R_i [(\mu, \zeta) \leftarrow (\mu_b, \mu_b^2)] \begin{pmatrix} \cos(\phi(\mu)) & -\sin(\phi(\mu)) \\ s \sin(\phi(\mu)) & s \cos(\phi(\mu)) \end{pmatrix} \left[\begin{pmatrix} \mathcal{C}_{i/j}^{Y/\Gamma,e} \\ \mathcal{C}_{i/j}^{Y/\Gamma,o} \end{pmatrix} \otimes f_j^{[\Gamma]} \right] (\mu_b, \mu_b^2), \quad (71)$$

in which the T-parity of $\mathbb{F}_i^{[Y],e}$ and $\mathbb{F}_i^{[Y],o}$ is explicitly preserved under evolution and matching.

Finally, we point out that GTMDs in momentum (\mathbf{k}_T) space can be obtained by Fourier transforming Eq. (71) w.r.t. the transverse displacement \mathbf{b} . Care must be taken when taking the Fourier transform to include also possible \mathbf{b} -dependent factors that appear in the decomposition of the relevant correlators. Therefore, the inversion of GTMDs from \mathbf{b} to \mathbf{k}_T space will generally read:

$$\hat{\mathbb{F}}_i^{[Y]}(x, \xi, \mathbf{k}_T, \Delta_T; \mu, \zeta) = \int d^2\mathbf{b} e^{-i\mathbf{b}\cdot\mathbf{k}_T} f(\mathbf{b}) \mathbb{F}_i^{[Y]}(x, \xi, \mathbf{b}, \Delta_T; \mu, \zeta), \quad (72)$$

where the factor $f(\mathbf{b})$ can be read off from Eqs. (27), (28), (29), and (30). More details on the numerical implementation of the Fourier transform in Eq. (72) for the specific GTMDs to be treated in Sec. 6 can be found in App. B.

⁶Note that setting $\mu = \mu_b$ in Eq. (11) causes all explicit logarithms in the one-loop matching functions in Eq. (14) to vanish.

⁷Note that an imaginary part is only present in the functions $\mathcal{C}_{i/g}^{Y/\Gamma}$, while $\mathcal{C}_{i/q}^{Y/\Gamma}$ are real (see Tab. 5). In other words, the imaginary part of the GTMDs generated by matching comes exclusively from gluon GPD channels.

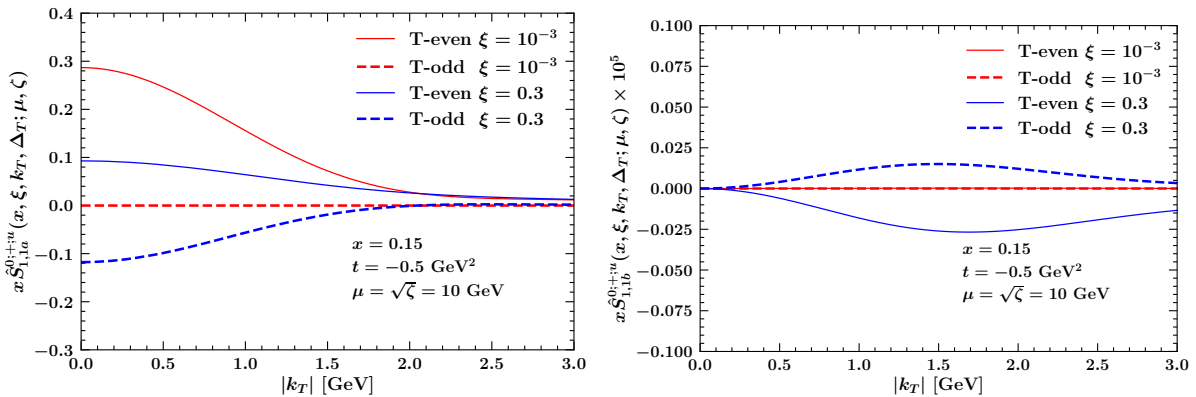


Figure 1: The GTMDs $\hat{S}_{1,1a}^{0;+;u}$ (left) and $\hat{S}_{1,1b}^{0;+;u}$ (right) plotted as functions of $|\mathbf{k}_T|$ at $x = 0.15$ and $\mu = \sqrt{\zeta} = 10$ GeV. Two different values of ξ are considered: $\xi = 10^{-3} < x$ (red curves) which probes the DGLAP region, and $\xi = 0.3 > x$ (blue curves) which instead probes the ERLB region. T-even and T-odd components are shown separately as solid and dashed curves, respectively. The plot for $\hat{S}_{1,1b}^{0;+;u}$ is magnified by a factor of 10^5 for presentation purposes.

6 Numerical results

In this section, we present a numerical implementation of the results obtained in the previous sections. In order to assess the magnitude of the T-even/T-odd mixing effect caused by evolution (Eq. (67)) and matching (Eq. (70)), we present a selection of numerical results for the GTMDs $S_{1,1a}^{0;+;q}$ and $S_{1,1b}^{0;+;q}$. These distributions are defined through Eq. (27) and match on GPDs as in Eqs. (33) and (34). Since we will only present results in momentum space, all GTMDs are Fourier transformed using Eq. (72) (see also App. B). Before moving to show our results, several general remarks are in order.

As no phenomenologically accurate extractions of the non-perturbative part of GTMDs are currently available, we resorted to using the forward TMD extraction of Ref. [61]. Moreover, no reliable models for the linearly polarised gluon GPDs \tilde{H}_T^g , E_T^g , and \tilde{E}_T^g currently exist. In their place, we used a scaled-down version of the corresponding unpolarised and longitudinally polarised GPDs, *i.e.* $\tilde{H}_T^g = c\tilde{H}^g$, $E_T^g = cE^g$, $\tilde{E}_T^g = c\tilde{E}^g$ with c arbitrarily chosen to be 10^{-1} , for which we used the Goloskokov-Kroll (GK) model [62–64]. As far as the perturbative accuracy is concerned, combining in Eq. (71) one-loop matching functions with anomalous dimensions computed at the appropriate perturbative order, allowed us to achieve next-to-next-to-leading-logarithmic (NNLL) accurate GTMDs [30, 61]. Concerning kinematics, since the proton mass M explicitly enters the matching expressions for GTMDs on GPDs, the momentum transfer $t = \Delta^2$ is subject to the following constraint:

$$|t| \geq |t_{\min}| = \frac{4M^2\xi^2}{1 - \xi^2}. \quad (73)$$

Assuming $M \simeq 1$ GeV, as appropriate for protons, in the following we will show results at $t = -0.5$ GeV², which in turn implies that $\xi \lesssim 0.35$. Moreover, one needs to specify the angle $\theta_{k\Delta}$ between the parton transverse momentum \mathbf{k}_T and the transverse component $\mathbf{\Delta}_T$ of the proton momentum transfer (see App. B). We set it to $\theta_{k\Delta} = 0$ for $\hat{S}_{1,1a}^{0;+;u}$ and to $\theta_{k\Delta} = \pi/4$ for $\hat{S}_{1,1b}^{0;+;u}$, which maximises the effect of the mixing between U and T channels.

We point out that the numerical results presented below were obtained using publicly available codes. Specifically, the GK model for the GPDs at the initial scale $\mu_0 = 2$ GeV is provided by PARTONS [65]; their collinear evolution as well as the perturbative ingredients relevant to matching and evolution are provided by APFEL++ [66, 67]; the non-perturbative components as well as the Fourier transform of GTMDs are provided by NangaParbat [61].

Fig. 1 displays the behavior of the up-quark GTMDs $\hat{S}_{1,1a}^{0;+;u}$ (left plot) and $\hat{S}_{1,1b}^{0;+;u}$ (right plot) as functions of $|\mathbf{k}_T|$ at $x = 0.15$ and $\mu = \sqrt{\zeta} = 10$ GeV for two different values of ξ . These values were chosen such that the first ($\xi = 10^{-3} < x$, red curves) corresponds to the DGLAP

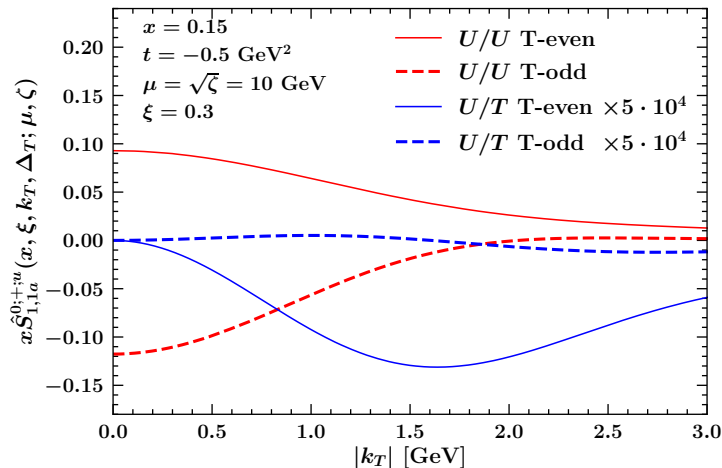


Figure 2: The T-even (solid curves) and T-odd (dashed curves) components to the GTMD $\hat{S}_{1,1a}^{0;+;u}$ as functions of $|k_T|$ at $x = 0.15$, $\xi = 0.3$, and $\mu = \sqrt{\zeta} = 10$ GeV. Each component is further separated into U/U (red curves) and U/T (blue curves) contributions.

region, while the second ($\xi = 0.3 > x$, blue curves) probes the ERBL region. T-even and T-odd contributions to both GTMDs are shown separately as solid and dashed curves, respectively. The curves for $\hat{S}_{1,1b}^{0;+;u}$ are multiplied by a factor of 10^5 to make them comparable in size with $\hat{S}_{1,1a}^{0;+;u}$. First, we note that, consistently with Eq. (71), T-odd contributions are identically zero in the DGLAP regions (see red dashed curves). In the ERBL region, the T-even component generally dominates for both distributions, though the T-odd contribution remains non-negligible. This aligns with the expectation that T-odd terms are suppressed by a power of α_s relative to their T-even counterparts. The suppression of $\hat{S}_{1,1b}^{0;+;u}$ compared to $\hat{S}_{1,1a}^{0;+;u}$ can be partially attributed to the same reasoning, along with the factor $c = 10^{-1}$, which suppresses linearly polarised gluon GPDs relative to their unpolarised and longitudinally polarised counterparts. However, this alone does not account for the full factor of 10^5 , which is primarily due to the effect of the matching functions. However, we point out that this suppression does not have any direct implications for the orbital angular momentum distribution [36, 37], since, as evident from Eq. (34), the matching is proportional to Δ_T and hence does not contribute to the orbital angular momentum distribution (see Eq. (28) of Ref. [36]).

As discussed in Sec. 3, each GTMD polarisation receives contributions from different GPDs polarisations. Indeed, from Eq. (33) we see that the unpolarised GTMD $\hat{S}_{1,1a}^{0;+;u}$ gets contributions both from unpolarised (U/U channel) and transversely/linearly polarised (U/T channel) GPDs. It is therefore interesting to examine their relative importance. To this purpose, in Fig. 2 we display U/U (red curves) and U/T (blue curves) contributions to $\hat{S}_{1,1a}^{0;+;u}$ for both T-even (solid curves) and T-odd (dashed curves) components. The same settings as in Fig. 1 are used but selecting $\xi = 0.3$. Moreover, the U/T contributions are multiplied by a factor of $5 \cdot 10^4$ to make them comparable in size to the U/U contributions. The suppression of the U/T channel relative to the U/U channel can be partially attributed to its suppression by a power of α_s and that linearly polarised gluon GPDs are a factor of $c = 10^{-1}$ smaller than their unpolarised/longitudinally-polarised counterparts. However, the suppression observed in Fig. 2 is stronger than expected and can again be traced back to the effect of the matching functions. Additionally, we find that the T-odd contribution is comparable in magnitude to the T-even one, emphasizing the need to account for T-odd effects in any future phenomenological study of GTMDs.

Finally, we investigate the mechanism through which T-odd effects are generated. As argued above, two different sources of T-odd effects are at play: matching and evolution. It is therefore insightful to compare their relative contributions. To this end, Fig. 3 displays the ratio $\hat{S}_{1,1a}^{0;+;u,o}/\hat{S}_{1,1a}^{0;+;u,e}$ as a function of $|k_T|$, with the rotation matrix in Eq.(71) set to unity. This effectively disables the evolution-induced T-odd effects, isolating those generated by matching. The same kinematic setup as in Fig. 2 is used. The results indicate that the ratio remains close

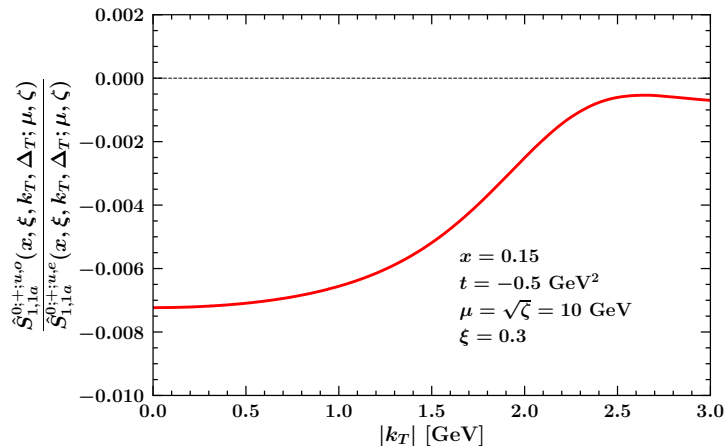


Figure 3: Ratio between the T-odd and T-even contributions to $\hat{S}_{1,1a}^{0;+;u}$ as a function of $|k_T|$ obtained by replacing the rotation matrix in Eq. (71) with the identity matrix. This modification ensures that matching is the sole source of T-odd effects.

to zero for all values of $|k_T|$ considered, implying that matching-induced T-odd effects contribute less than 1% of the total. This proves that evolution is the dominant source of T-odd effects.

In conclusion, the exploratory numerical study presented above may be useful for future phenomenological studies in that it exposes various interesting features of GTMDs. We showed how different GPD polarisations contribute to a given GTMD polarisation, focussing here on unpolarised GTMDs only. Additionally, we analysed the interplay between T-even and T-odd components, showing that while T-odd contributions remain small, they are generally non-negligible in the ERBL region. In this respect, we also demonstrated that by far the most important contribution to the generation of T-odd effects is evolution.

7 Conclusions

In this work, we have presented the one-loop, *i.e.* $\mathcal{O}(\alpha_s)$, corrections to the matching functions for all of the twist-two GTMDs of the proton. These matching functions are an important ingredient in any accurate phenomenological study of the internal structure of the proton. In fact, they allow one to reconstruct GTMDs in terms of GPDs in the region of small partonic transverse separations \mathbf{b} , or equivalently large partonic transverse momenta \mathbf{k}_T . This is analogous to the matching of TMDs onto collinear PDFs, which is routinely exploited in extractions of TMDs from experimental data. In fact, in the largely unexplored realm of GTMDs, their matching relations on GPDs turn out to be even more important to achieve a realistic reconstruction of these multidimensional objects.

GTMDs are more complex objects than their unskewed counterparts, *i.e.* TMDs. Indeed, GTMDs feature a number of novel aspects compared to TMDs, which we highlighted here for the first time. In Sec. 3, we demonstrated that the matching pattern of GTMDs on GPDs is much richer than that of TMDs. More specifically, we showed that for any given GTMD polarisation multiple GPD polarisations may contribute (see Tab. 1). We also demonstrated that one-loop GTMD matching functions on gluon GPDs in the ERBL region ($\xi > x$) develop an imaginary part proportional to the direction of the Wilson line, $s = \pm 1$, which contributes to the perturbative mixing of T-even and T-odd GTMDs (see also Eq. (70)). In Sec. (4), leveraging existing results, we obtained a parametrisation of the twist-two GTMD correlators in terms of GTMD distributions in \mathbf{b} space (suitable for matching) and presented their matching on standard twist-two GPDs at small $|\mathbf{b}|$. In Sec. 5, we focused on the evolution of GTMDs. We proved that the solution of the evolution equations, more specifically the one w.r.t. to μ , is responsible for yet another source of T-even/T-odd mixing (see Eq. (67)). Combining perturbative matching and evolution, we obtained Eq. (71), which allows for a full reconstruction of GTMDs in terms of GPDs and a number of perturbatively computable quantities. In this formula, a particularly important role is played by matching functions whose full set of one-loop

corrections were computed here for the first time.

In Sec. 6, we presented a selection of numerical results with the purpose of quantitatively illustrating the effect of polarisation as well as that of T-even/T-odd mixing when reconstructing GTMDs. We found that polarisation mixing plays an important role in the sense that the contribution of off-diagonal GPDs, *i.e.* GPDs whose polarisation differs from that of the GTMD they match on, is non-negligible. As far as the T-even/T-odd mixing is concerned, we found that the mixing produced by evolution is far larger than the mixing produced by matching.

We finally point out that, modulo the reliability of GPDs and possible non-perturbative effects, the GTMDs reconstructed in Sec. 6 should be regarded as realistic in that they encode the full QCD-driven complexity that emerges from perturbative matching and evolution. Therefore, our results provide a crucial foundation for future phenomenological studies of GTMDs and their role in understanding the proton multi-dimensional structure.

Acknowledgements

The authors are grateful to M. Diehl for a critical reading of the manuscript. The work of M.G.E. is supported by the State Research Agency through the grants PCI2022-132984, PID2022-136510NB-C33 and CNS2022-135186, and by the Basque Government through the grant IT1628-22. The work of S.R. is supported by the German Science Foundation (DFG), grant number 409651613 (Research Unit FOR 2926), subproject 430915355. O. dR. is supported by the MIU (Ministerio de Universidades, Spain) fellowship FPU20/03110. Additionally, O. dR. thanks DESY for its hospitality during his three-month research stay, funded by the MIU mobility grant EST24/00197, during which part of this work was carried out.

A On the presence of imaginary contributions

A.1 Imaginary part in the evolution

The imaginary part present in the evolution equation w.r.t. μ in Eq. (61) can be explained in terms of the UV renormalisation constant for the generic twist-one operator (*e.g.*, see Eq. (8.22) of Ref. [68]). In the quark case, its one-loop expression in $4 - 2\epsilon$ dimensions reads:

$$Z\left(\frac{\delta^+}{k^+}\right) = 1 + \left(\frac{\alpha_s}{4\pi}\right) \frac{C_F}{\epsilon} \left(\frac{3}{2} + 2 \log\left(\frac{\delta^+}{isk^+}\right)\right), \quad (74)$$

where δ^+ is the (dimension-full) regulator of rapidity divergences (see Refs. [58, 69]), $s = \pm 1$ identifies the direction of the Wilson line, and k^+ is the momentum of the external parton. The UV renormalisation for the whole twist-two operator associated with the GTMDs is obtained as:

$$Z^\dagger\left(\frac{\delta^+}{k_1^+}\right) Z\left(\frac{\delta^+}{k_2^+}\right), \quad (75)$$

where k_1^+ (k_2^+) is the momentum associated with the left (right) field in Eqs. (3) and (4), which we parametrise as $k_1^+ = (1 - \kappa)xp^+$ ($k_2^+ = (1 + \kappa)xp^+$). Here, we stress once again that we can always reduce ourselves to the case of $x, \xi \geq 0$, which implies $\kappa \geq 0$. Therefore, the one-loop UV renormalisation constant takes the form:

$$\begin{aligned} Z^\dagger\left(\frac{\delta^+}{(1 - \kappa)xp^+}\right) Z\left(\frac{\delta^+}{(1 + \kappa)xp^+}\right) &= 1 + \left(\frac{\alpha_s}{4\pi}\right) \frac{2C_F}{\epsilon} \left(\frac{3}{2} + 2 \log\left(\frac{\delta^+}{xp^+}\right) - \log(|1 - \kappa^2|)\right. \\ &\quad \left. - \log(-is \operatorname{sign}(1 - \kappa)) - \log(is \operatorname{sign}(1 + \kappa))\right). \end{aligned} \quad (76)$$

The term $\log(|1 - \kappa^2|)$ in the equation above is precisely the same that appears in the GTMD evolution equation w.r.t. μ in Eq. (61). The terms in the second line, instead, generate the imaginary part. Indeed, we have:

$$-\log(-is \operatorname{sign}(1 + \kappa)) - \log(is \operatorname{sign}(1 - \kappa)) = -i\pi s\theta(\kappa - 1), \quad (77)$$

such that the imaginary part vanishes in the DGLAP region ($\kappa < 1$), while it survives in the ERLB region ($\kappa > 1$).

Now we can complete the renormalization of the GTMD operator by introducing the renormalization of the rapidity divergences, to obtain:

$$\mathcal{F}_{q/H;bare}^{[Y]} = R\left(b^2, \frac{\delta^+}{\nu^+}\right) Z^\dagger\left(\frac{\delta^+}{(1-\kappa)xp^+}\right) Z\left(\frac{\delta^+}{(1+\kappa)xp^+}\right) \mathcal{F}_{q/H}^{[Y]}(\nu^+, \mu), \quad (78)$$

where the scale ν^+ is introduced as a reference scale to subtract rapidity divergences. The last step is to divide out the (square root of the) soft factor⁸. To this end, one can write the soft factor as (where $\nu^2 = 2\nu^+\nu^-$):

$$\begin{aligned} S(b^2, 2\delta^+\delta^-) &= Z_S\left(\frac{2\delta^+\delta^-}{\mu^2}\right) R\left(b^2, \frac{\delta^+}{\nu^+}\right) R\left(b^2, \frac{\delta^-}{\nu^-}\right) S_0(b^2, \nu^2) \\ &= \left[R\left(b^2, \frac{\delta^+}{\nu^+}\right) \sqrt{Z_S\left(\frac{\nu^2}{\mu^2}\right) Z_R\left(\frac{\delta^+}{\nu^+}\right) S_0(b^2, \nu^2)} \right] \\ &\quad \times \left[R\left(b^2, \frac{\delta^-}{\nu^-}\right) \sqrt{Z_S\left(\frac{\nu^2}{\mu^2}\right) Z_R\left(\frac{\delta^-}{\nu^-}\right) S_0(b^2, \nu^2)} \right], \end{aligned} \quad (79)$$

where S_0 is free from UV and rapidity divergences and Z_S is the UV renormalization for the soft factor:

$$Z_S\left(\frac{2\delta^+\delta^-}{\mu^2}\right) \equiv Z_S\left(\frac{\nu^2}{\mu^2}\right) Z_R\left(\frac{\delta^+}{\nu^+}\right) Z_R\left(\frac{\delta^-}{\nu^-}\right). \quad (80)$$

Referring to the pion-nucleon double Drell-Yan process detailed in Ref. [50], the first term in the second line is divided out from the proton GTMD, the second term in the second line is divided out from the pion light-cone wave function. Finally, we can write:

$$\frac{\mathcal{F}_{q/H;bare}^{[Y]}}{R\left(b^2, \frac{\delta^+}{\nu^+}\right) \sqrt{Z_S\left(\frac{\nu^2}{\mu^2}\right) Z_R\left(\frac{\delta^+}{\nu^+}\right) S_0(b^2, \nu^2)}} = \mathbb{Z}\left(\frac{\xi}{x}, \frac{\mu^2}{\zeta}\right) \mathcal{F}_{q/H}^{[Y]}(\zeta, \mu), \quad (81)$$

where:

$$\mathbb{Z}\left(\frac{\xi}{x}, \frac{\mu^2}{\zeta}\right) = \frac{Z^\dagger\left(\frac{\delta^+}{(1-\kappa)xp^+}\right) Z\left(\frac{\delta^+}{(1+\kappa)xp^+}\right)}{\sqrt{Z_S\left(\frac{\nu^2}{\mu^2}\right) Z_R\left(\frac{\delta^+}{\nu^+}\right)}}, \quad (82)$$

and:

$$\mathcal{F}_{q/H}^{[Y]}(\zeta, \mu) = \frac{\mathcal{F}_{q/H}^{[Y]}(\nu^+, \mu)}{\sqrt{S_0(b^2, \nu^2)}}. \quad (83)$$

In the relations above, we introduced the rapidity scale ζ as:

$$\zeta = 2|k_1^+ k_2^+| \frac{\nu^-}{\nu^+} = 2(xp^+)^2 |1 - \kappa^2| \frac{\nu^-}{\nu^+}. \quad (84)$$

This scale cannot be fixed completely independently from the other components of the factorisation theorem, since it must satisfy the equality:

$$\zeta \bar{\zeta} = (Q_1^2)(Q_2^2), \quad (85)$$

where $Q_{1,2}^2$ are hard scales equal to the momenta of the two virtual bosons and $\bar{\zeta}$ has a similar definition for the light-cone wave function of the pion.

As a final remark, we stress that the emergence of the imaginary part in the UV renormalization factors is *not* an artifact of the specific regulator δ^+ . Regulating rapidity divergences using off-the-light-cone Wilson lines leads to the same result.⁹ For a more in-depth discussion about the intricacies of the definition of the rapidity scale, we refer to Refs. [17, 70].

⁸For the sake of illustration, we use a similar notation to Ref. [68], which we refer the reader for further details.

⁹Compare with the UV pole part of the one-loop coefficient function for quasi-TMD operators in Eq. (4.31) of Ref. [28].

A.2 Imaginary part in the residual function

We now discuss the terms $is\delta$ in the results of Tab. 1, which in turn give rise to an imaginary part in the matching functions through Eq. (21). In order to sketch how this imaginary part emerges, we first note that it is only present in matching functions that are to be convoluted with a gluon GPD. In the parton-in-parton approach and at leading twist, these matching functions can be obtained by computing matrix elements between *physical* gluon states. The computation of any such matching function necessarily boils down to evaluating matrix elements of this sort:

$${}_g \langle k_1 | A^j(x_1) A^i(x_2) | k_2 \rangle_g, \quad (86)$$

where the subscripts g indicate gluon states. To relate this matrix element to the gluon GPD in Eq. (6), we need to express it in terms of the field strength tensor F^{+i} . The simplest way to present the argument is to work in light-cone gauge $A^+ = 0$, equipped with appropriate boundary conditions:

$$\lim_{L \rightarrow s\infty} A^i(x + Ln) = 0. \quad (87)$$

Importantly, s has to be the same sign that determines the direction of the Wilson line in the GTMD correlator. Indeed, in order to reduce to unity the transverse gauge link at light-cone infinity involved in the GTMD correlator, $A^i(x + Ln)$ must vanish exactly when $L \rightarrow s\infty$. This allows us to write:

$$A^i(x) = \lim_{L \rightarrow s\infty} \int_L^0 d\sigma F^{+i}(x + \sigma n). \quad (88)$$

With a slight abuse of notation, Eq. (88) in momentum space becomes:

$$A^i(k) e^{-i(kx)} = F^{+i}(k) e^{-i(kx)} \int_{s\infty}^0 d\sigma e^{-i(k^+ - is\delta p^+) \sigma}, \quad (89)$$

where we performed the shift:¹⁰

$$k^+ \rightarrow k^+ - is\delta p^+, \quad (90)$$

with δ a small positive parameter. Evaluating the integral in σ , we obtain:

$$A^i(k) = \frac{i}{k^+ - i\delta s p^+} F^{+i}(k). \quad (91)$$

Using this identity in the momentum-space version of Eq. (86), we find:

$${}_g \langle k_1 | A^j(k_1) A^i(k_2) | k_2 \rangle_g = \frac{1}{k_2^+ - is\delta p^+} \frac{1}{k_1^+ + is\delta p^+} {}_g \langle k_1 | F^{+j}(k_1) F^{+i}(k_2) | k_2 \rangle_g, \quad (92)$$

which achieves the goal of rewriting the matrix element in Eq. (86) in a form compatible with the definition of gluon GPD in Eq. (6). As customary, the gluon momenta k_1 and k_2 can be chosen to have only non-vanishing $+$ components, which are parametrised as $k_1^+ = (1 - \eta)(x/y)p^+$ and $k_2^+ = (1 + \eta)(x/y)p^+$. The variable η denotes the ratio between skewness ξ and GPD partonic longitudinal momentum. This is a different variable from $\kappa = \xi/x$. Indeed, using Eq. (11) as a reference, one has that $\eta = \xi/(x/y) = \kappa y$. The consequence is that the matrix element in the l.h.s. of Eq. (92) will be proportional to the factor:

$$\frac{1}{1 - \kappa y + is\delta} \frac{1}{1 + \kappa y - is\delta}, \quad (93)$$

which is singular at $y = \pm 1/\kappa$. Note that we have extracted a factor $(x/y)p^+$ from each denominator without having to keep track of its sign in the imaginary part, since it is always possible to choose $x, y, \kappa > 0$. This has also the consequence of leaving only the singularity at $y = 1/\kappa$ inside the integration range, while pushing the singularity at $y = -1/\kappa$ outside of it.

¹⁰We dropped the shift in $e^{-i(kx)}$, since it is uninfluential for the argument and thus can be safely discarded.

Therefore, we can remove the regulator δ from the second factor in Eq. (93) and treat it as a regular function. Finally, using the identity:

$$\frac{1}{1 - \kappa y + i s \delta} = \text{PV} \left(\frac{1}{1 - \kappa y} \right) - i s \frac{\pi}{\kappa} \delta \left(y - \frac{1}{\kappa} \right), \quad (94)$$

valid for δ vanishingly small, we obtain the imaginary part in the matching functions in Eq. (21), which, crucially, is proportional to the Wilson-line direction s .

A similar argument also applies to the calculation of the one-loop GPD splitting functions $\mathcal{P}_{i/j}^{\Gamma, [0]}$ [56, 57] which appear in Eq. (14). However, it turns out that in this case the coefficient of $(1 - \kappa y + i s \delta)^{-1}$ vanishes, implying the absence of imaginary contributions related to the computation of matrix elements as in Eq. (86).

A.3 Vanishing imaginary part in the splitting functions

There is yet another possible source of imaginary contributions that may affect the one-loop splitting functions $\mathcal{P}_{i/j}^{\Gamma, [0]}$, namely the imaginary terms that emerge from the renormalisation of the twist-one operators discussed in Sec. A.1 (see Eq. (76)). We now review the proof that splitting functions are free of rapidity divergences for $\delta \rightarrow 0$. In the proof, we keep explicit track of the various imaginary parts, showing that they eventually cancel out leaving a real result. To do so, we limit to the unpolarised non-singlet splitting function $\mathcal{P}^{U, -, [0]}$ (all the others follow a similar pattern) and, without loss of generality, we assume a future-pointing Wilson line ($s = 1$). The starting point reads [56, 57]:

$$\mathcal{P}^{U, -, [0]}(y, \kappa) = \theta(1 - y) \mathcal{P}_1^{U, -, [0]}(y, \kappa) + \theta(\kappa - 1) \mathcal{P}_2^{U, -, [0]}(y, \kappa), \quad (95)$$

where:

$$\begin{aligned} \mathcal{P}_1^{U, -, [0]}(y, \kappa) &= p_{q/q}^U(y, \kappa) + p_{q/q}^U(y, -\kappa) \\ &+ \delta(1 - y) 2C_q \left[\frac{3}{2} + \log \left(\frac{-i\delta}{1 + \kappa} \right) + \log \left(\frac{-i\delta}{1 - \kappa} \right) \right], \\ \mathcal{P}_2^{U, -, [0]}(y, \kappa) &= -p_{q/q}^U(y, -\kappa) + p_{q/q}^U(-y, -\kappa). \end{aligned} \quad (96)$$

We can read off $p_{q/q}^U$ from Ref. [57]:

$$p_{q/q}^U(y, \kappa) = C_F \frac{(1 + \kappa)(1 - y + 2\kappa y)}{\kappa(1 + \kappa y)(1 - y - i\delta)}. \quad (97)$$

Since $\mathcal{P}_1^{U, -, [0]}$ in Eq. (95) is accompanied by $\theta(1 - y)$, the singularity of $p_{q/q}^U$ at $y = 1$ is an end-point one. In this case, we use the identity:

$$\frac{1}{1 - y - i\delta} \rightarrow \left(\frac{1}{1 - y} \right)_+ - \delta(1 - y) \log(-i\delta), \quad (98)$$

where the +-prescription is defined as in Eq. (40) of Ref. [57], so that:

$$p_{q/q}^U(y, \kappa) = C_F \frac{(1 + \kappa)(1 - y + 2\kappa y)}{\kappa(1 + \kappa y)} \left(\frac{1}{1 - y} \right)_+ - \delta(1 - y) 2C_F \log(-i\delta). \quad (99)$$

When inserted into the first equation in Eq. (96), this produces:

$$\mathcal{P}_1^{U, -, [0]}(y, \kappa) = p_{q/q}^U(y, \kappa) + p_{q/q}^U(y, -\kappa) + \delta(1 - y) 2C_F \left[\frac{3}{2} - \log(1 + \kappa) - \log(1 - \kappa) \right], \quad (100)$$

where $p_{q/q}^U$ here is understood to have the factor $(1 - y)^{-1}$ replaced by $(1 - y)_+^{-1}$. This leaves us with a term proportional to $\log(1 - \kappa)$ that, for $\kappa > 1$ (*i.e.* in the ERBL region), becomes complex.

If we now consider $\mathcal{P}_2^{U,-,[0]}$, the singularity at $y = 1$ is no longer an end-point one. This allows us to replace the factor $(1 - y - i\delta)^{-1}$ in Eq. (97) using Eq. (94) with $\kappa = 1$, so that:

$$p_{q/q}^U(y, -\kappa) = -C_F \frac{(1 - \kappa)(1 - y - 2\kappa y)}{\kappa(1 - \kappa y)} \text{PV} \left(\frac{1}{1 - y} \right) + i\pi\delta(1 - y)2C_F, \quad (101)$$

which gives:

$$\mathcal{P}_2^{U,-,[0]}(y, \kappa) = -p_{q/q}^U(y, -\kappa) + p_{q/q}^U(-y, -\kappa) - i\pi\delta(1 - y)2C_F, \quad (102)$$

where this time $p_{q/q}^U(y, -\kappa)$ has the factor $(1 - y)^{-1}$ replaced by $\text{PV}(1 - y)^{-1}$.

Now, if we take the combination in Eq. (95) using Eqs. (100) and (102), we see that the δ -function terms combine as follows:

$$2C_F \left[\frac{3}{2} - \log(1 + \kappa) - \log(1 - \kappa) - i\pi\theta(\kappa - 1) \right] = 2C_F \left[\frac{3}{2} - \log(|1 - \kappa^2|) \right], \quad (103)$$

which finally proves that the splitting function $\mathcal{P}^{U,-,[0]}$ is free of imaginary contributions, *i.e.* it is real.

B Fourier transformation

In this section, we work out explicitly two examples of Fourier transforms necessary to convert GTMD distributions from \mathbf{b} -space to \mathbf{k}_T -space. We consider the GTMDs $S_{1,1a}^{0,+;i}$ and $S_{1,1b}^{0,+;i}$ defined in Eq. (27) and showed in Sec. 6 for $i = q$. In the first case, we need to compute the integral:

$$\hat{S}_{1,1a}^{0,+;i}(x, \xi, \mathbf{k}_T, \mathbf{\Delta}_T; \mu, \zeta) = \int d^2\mathbf{b} e^{-i\mathbf{b}\cdot\mathbf{k}_T} S_{1,1a}^{0,+;i}(x, \xi, \mathbf{b}, \mathbf{\Delta}_T; \mu, \zeta). \quad (104)$$

A \mathbf{b} -dependent structure comes from the last line of Eqs. (33) and (45). If we combine these equations with Eq. (62), which encodes the evolution of GTMDs, we can write:

$$\begin{aligned} S_{1,1a}^{0,+;i}(x, \xi, \mathbf{b}, \mathbf{\Delta}_T; \mu, \zeta) &= \mathcal{R}_i [(\mu, \zeta) \leftarrow (\mu_b, \mu_b^2)] f_1^i(x, \xi, \mathbf{\Delta}_T; \mu_b) \\ &- \mathcal{R}_i [(\mu, \zeta) \leftarrow (\mu_b, \mu_b^2)] \frac{2(\mathbf{b} \cdot \mathbf{\Delta}_T)^2 - \mathbf{b}^2 \mathbf{\Delta}_T^2}{4\mathbf{b}^2 M^2} f_2^i(x, \xi, \mathbf{\Delta}_T; \mu_b), \end{aligned} \quad (105)$$

where f_1 and f_2 can be read off from Eqs. (33) and (45) and are given by:

$$\begin{aligned} f_1^i(x, \xi, \mathbf{\Delta}_T; \mu_b) &= C_{i/q}^{U/U} \otimes [(1 - \xi^2)H^q - \xi^2 E^q](x, \xi, \mathbf{\Delta}_T; \mu_b) \\ &+ C_{i/g}^{U/U} \otimes [(1 - \xi^2)H^g - \xi^2 E^g](x, \xi, \mathbf{\Delta}_T; \mu_b), \\ f_2^i(x, \xi, \mathbf{\Delta}_T; \mu_b) &= C_{i/g}^{U/T} \otimes [E_T^g - \xi \tilde{E}_T^g + 2\tilde{H}_T^g](x, \xi, \mathbf{\Delta}_T; \mu_b). \end{aligned} \quad (106)$$

It is generally not possible to compute the Fourier transform in Eq. (104) fully analytically. However, it can be reduced to a Hankel transform, which can be evaluated numerically. This leads to:

$$\begin{aligned} \hat{S}_{1,1a}^{0,+;i}(x, \xi, \mathbf{k}_T, \mathbf{\Delta}_T; \mu, \zeta) &= 2\pi \int_0^\infty d|\mathbf{b}| |\mathbf{b}| J_0(|\mathbf{b}| |\mathbf{k}_T|) \mathcal{R}_i [(\mu, \zeta) \leftarrow (\mu_b, \mu_b^2)] f_1^i(x, \xi, \mathbf{\Delta}_T; \mu_b) \\ &+ 2\pi \frac{2(\mathbf{k}_T \cdot \mathbf{\Delta}_T)^2 - \mathbf{k}_T^2 \mathbf{\Delta}_T^2}{4M^2 \mathbf{k}_T^2} \int_0^\infty d|\mathbf{b}| |\mathbf{b}| J_2(|\mathbf{b}| |\mathbf{k}_T|) \mathcal{R}_i [(\mu, \zeta) \leftarrow (\mu_b, \mu_b^2)] f_2^i(x, \xi, \mathbf{\Delta}_T; \mu_b). \end{aligned} \quad (107)$$

The prefactor of the term in second line of the equation above can be rewritten as follows:

$$2\pi \frac{2(\mathbf{k}_T \cdot \mathbf{\Delta}_T)^2 - \mathbf{k}_T^2 \mathbf{\Delta}_T^2}{4M^2 \mathbf{k}_T^2} = 2\pi \left[(1 - \xi^2) \frac{(-t)}{4M^2} - \xi^2 \right] \cos(2\theta_{k\Delta}), \quad (108)$$

being $t = \Delta^2 < 0$ and $\theta_{k\Delta}$ the angle between \mathbf{k}_T and Δ_T .

In the case of $S_{1,1b}^{0;+;i}$, the relevant term to transform is:

$$\hat{S}_{1,1b}^{0;+;i}(x, \xi, \mathbf{k}_T, \Delta_T; \mu, \zeta) \equiv \int d^2\mathbf{b} e^{-i(\mathbf{b}\cdot\mathbf{k}_T)} \frac{i\varepsilon_T^{b\Delta_T}}{M|\mathbf{b}|} S_{1,1b}^{0;+;i}(x, \xi, \mathbf{b}, \Delta_T; \mu, \zeta). \quad (109)$$

The GTMDs in \mathbf{b} -space from Eqs. (34) and (46) are given by:

$$S_{1,1b}^{0;+;i}(x, \xi, \mathbf{b}, \Delta_T; \mu, \zeta) = \mathcal{R}_i [(\mu, \zeta) \leftarrow (\mu_b, \mu_b^2)] \frac{(\mathbf{b}\cdot\Delta_T)}{2M|\mathbf{b}|} f_3^i(x, \xi, \Delta_T; \mu_b), \quad (110)$$

where f_3 reads:

$$f_3^i(x, \xi, \Delta_T; \mu_b) = C_{i/g}^{U/T} \otimes [\xi E_T^g - \tilde{E}_T^g] (x, \xi, \Delta_T; \mu_b). \quad (111)$$

Therefore, its Fourier transform yields:

$$\begin{aligned} \hat{S}_{1,1b}^{0;+;i}(x, \xi, \mathbf{k}_T, \Delta_T; \mu, \zeta) &= -\frac{\pi}{M^2} \frac{i\varepsilon_T^{k_T\Delta_T}(\mathbf{k}_T\cdot\Delta_T)}{\mathbf{k}_T^2} \\ &\int_0^\infty d|\mathbf{b}| |\mathbf{b}| J_2(|\mathbf{b}||\mathbf{k}_T|) \mathcal{R}_i [(\mu, \zeta) \leftarrow (\mu_b, \mu_b^2)] f_3^i(x, \xi, \Delta_T; \mu_b), \end{aligned} \quad (112)$$

where the prefactor can be conveniently expressed as follows:

$$-\frac{\pi}{M^2} \frac{i\varepsilon_T^{k_T\Delta_T}(\mathbf{k}_T\cdot\Delta_T)}{\mathbf{k}_T^2} = -2\pi i \left[(1 - \xi^2) \frac{(-t)}{4M^2} - \xi^2 \right] \sin(2\theta_{k\Delta}). \quad (113)$$

References

- [1] A. Bacchetta, F. Delcarro, C. Pisano, M. Radici, and A. Signori, “Extraction of partonic transverse momentum distributions from semi-inclusive deep-inelastic scattering, Drell-Yan and Z-boson production,” *JHEP*, vol. 06, p. 081, 2017. [Erratum: *JHEP* 06, 051 (2019)].
- [2] I. Scimemi and A. Vladimirov, “Analysis of vector boson production within TMD factorization,” *Eur. Phys. J. C*, vol. 78, no. 2, p. 89, 2018.
- [3] I. Scimemi and A. Vladimirov, “Non-perturbative structure of semi-inclusive deep-inelastic and Drell-Yan scattering at small transverse momentum,” *JHEP*, vol. 06, p. 137, 2020.
- [4] A. Bacchetta, V. Bertone, C. Bissolotti, G. Bozzi, M. Cerutti, F. Piacenza, M. Radici, and A. Signori, “Unpolarized transverse momentum distributions from a global fit of Drell-Yan and semi-inclusive deep-inelastic scattering data,” *JHEP*, vol. 10, p. 127, 2022.
- [5] J. Cammarota, L. Gamberg, Z.-B. Kang, J. A. Miller, D. Pitonyak, A. Prokudin, T. C. Rogers, and N. Sato, “Origin of single transverse-spin asymmetries in high-energy collisions,” *Phys. Rev. D*, vol. 102, no. 5, p. 054002, 2020.
- [6] M. G. Echevarria, Z.-B. Kang, and J. Terry, “Global analysis of the Sivers functions at NLO+NNLL in QCD,” *JHEP*, vol. 01, p. 126, 2021.
- [7] M. Bury, F. Hautmann, S. Leal-Gomez, I. Scimemi, A. Vladimirov, and P. Zurita, “PDF bias and flavor dependence in TMD distributions,” *JHEP*, vol. 10, p. 118, 2022.
- [8] M. Cerutti, L. Rossi, S. Venturini, A. Bacchetta, V. Bertone, C. Bissolotti, and M. Radici, “Extraction of pion transverse momentum distributions from Drell-Yan data,” *Phys. Rev. D*, vol. 107, no. 1, p. 014014, 2023.
- [9] V. Moos, I. Scimemi, A. Vladimirov, and P. Zurita, “Extraction of unpolarized transverse momentum distributions from fit of Drell-Yan data at N⁴LL.” 5 preprint.

- [10] J. Collins, *Foundations of Perturbative QCD*, vol. 32 of *Cambridge Monographs on Particle Physics, Nuclear Physics and Cosmology*. Cambridge University Press, 7 2023.
- [11] V. Moos and A. Vladimirov, “Calculation of transverse momentum dependent distributions beyond the leading power,” *JHEP*, vol. 12, p. 145, 2020.
- [12] M. A. Ebert, B. Mistlberger, and G. Vita, “TMD Fragmentation Functions at N³LO,” *JHEP*, vol. 07, p. 121, 2021.
- [13] M.-x. Luo, T.-Z. Yang, H. X. Zhu, and Y. J. Zhu, “Unpolarized quark and gluon TMD PDFs and FFs at N³LO,” *JHEP*, vol. 06, p. 115, 2021.
- [14] D. Gutierrez-Reyes, I. Scimemi, and A. Vladimirov, “Transverse momentum dependent transversely polarized distributions at next-to-next-to-leading-order,” *JHEP*, vol. 07, p. 172, 2018.
- [15] D. Gutierrez-Reyes, S. Leal-Gomez, I. Scimemi, and A. Vladimirov, “Linearly polarized gluons at next-to-next-to leading order and the Higgs transverse momentum distribution,” *JHEP*, vol. 11, p. 121, 2019.
- [16] D. Gutiérrez-Reyes, I. Scimemi, and A. A. Vladimirov, “Twist-2 matching of transverse momentum dependent distributions,” *Phys. Lett. B*, vol. 769, pp. 84–89, 2017.
- [17] M. G. A. Buffing, M. Diehl, and T. Kasemets, “Transverse momentum in double parton scattering: factorisation, evolution and matching,” *JHEP*, vol. 01, p. 044, 2018.
- [18] A. Bacchetta and A. Prokudin, “Evolution of the helicity and transversity Transverse-Momentum-Dependent parton distributions,” *Nucl. Phys. B*, vol. 875, pp. 536–551, 2013.
- [19] K. Kanazawa, Y. Koike, A. Metz, D. Pitonyak, and M. Schlegel, “Operator Constraints for Twist-3 Functions and Lorentz Invariance Properties of Twist-3 Observables,” *Phys. Rev. D*, vol. 93, no. 5, p. 054024, 2016.
- [20] I. Scimemi and A. Vladimirov, “Matching of transverse momentum dependent distributions at twist-3,” *Eur. Phys. J. C*, vol. 78, no. 10, p. 802, 2018.
- [21] S. Meissner, A. Metz, and K. Goeke, “Relations between generalized and transverse momentum dependent parton distributions,” *Phys. Rev. D*, vol. 76, p. 034002, 2007.
- [22] D. Boer, P. J. Mulders, and F. Pijlman, “Universality of T odd effects in single spin and azimuthal asymmetries,” *Nucl. Phys. B*, vol. 667, pp. 201–241, 2003.
- [23] X. Ji, J.-W. Qiu, W. Vogelsang, and F. Yuan, “A Unified picture for single transverse-spin asymmetries in hard processes,” *Phys. Rev. Lett.*, vol. 97, p. 082002, 2006.
- [24] J. Zhou, F. Yuan, and Z.-T. Liang, “Transverse momentum dependent quark distributions and polarized Drell-Yan processes,” *Phys. Rev. D*, vol. 81, p. 054008, 2010.
- [25] L.-Y. Dai, Z.-B. Kang, A. Prokudin, and I. Vitev, “Next-to-leading order transverse momentum-weighted Sivers asymmetry in semi-inclusive deep inelastic scattering: the role of the three-gluon correlator,” *Phys. Rev. D*, vol. 92, no. 11, p. 114024, 2015.
- [26] I. Scimemi, A. Tarasov, and A. Vladimirov, “Collinear matching for Sivers function at next-to-leading order,” *JHEP*, vol. 05, p. 125, 2019.
- [27] F. Rein, S. Rodini, A. Schäfer, and A. Vladimirov, “Sivers, Boer-Mulders and worm-gear distributions at next-to-leading order,” *JHEP*, vol. 01, p. 116, 2023.
- [28] S. Rodini and A. Vladimirov, “Definition and evolution of transverse momentum dependent distribution of twist-three,” *JHEP*, vol. 08, p. 031, 2022. [Erratum: *JHEP* 12, 048 (2022)].

- [29] S. Rodini, A. C. Alvaro, and B. Pasquini, “Collinear matching for next-to-leading power transverse-momentum distributions,” *Phys. Lett. B*, vol. 845, p. 138163, 2023.
- [30] V. Bertone, “Matching generalised transverse-momentum-dependent distributions onto generalised parton distributions at one loop,” *Eur. Phys. J. C*, vol. 82, no. 10, p. 941, 2022.
- [31] S. Meissner, A. Metz, M. Schlegel, and K. Goeke, “Generalized parton correlation functions for a spin-0 hadron,” *JHEP*, vol. 08, p. 038, 2008.
- [32] S. Meissner, A. Metz, and M. Schlegel, “Generalized parton correlation functions for a spin-1/2 hadron,” *JHEP*, vol. 08, p. 056, 2009.
- [33] C. Lorcé and B. Pasquini, “Structure analysis of the generalized correlator of quark and gluon for a spin-1/2 target,” *JHEP*, vol. 09, p. 138, 2013.
- [34] K. Kanazawa, C. Lorcé, A. Metz, B. Pasquini, and M. Schlegel, “Twist-2 generalized transverse-momentum dependent parton distributions and the spin/orbital structure of the nucleon,” *Phys. Rev. D*, vol. 90, no. 1, p. 014028, 2014.
- [35] M. G. Echevarria, A. Idilbi, K. Kanazawa, C. Lorcé, A. Metz, B. Pasquini, and M. Schlegel, “Proper definition and evolution of generalized transverse momentum dependent distributions,” *Phys. Lett. B*, vol. 759, pp. 336–341, 2016.
- [36] C. Lorce and B. Pasquini, “Quark Wigner Distributions and Orbital Angular Momentum,” *Phys. Rev. D*, vol. 84, p. 014015, 2011.
- [37] Y. Hatta, “Notes on the orbital angular momentum of quarks in the nucleon,” *Phys. Lett. B*, vol. 708, pp. 186–190, 2012.
- [38] Y. Hagiwara, Y. Hatta, and T. Ueda, “Wigner, Husimi, and generalized transverse momentum dependent distributions in the color glass condensate,” *Phys. Rev. D*, vol. 94, no. 9, p. 094036, 2016.
- [39] Y. Hagiwara, Y. Hatta, R. Pasechnik, M. Tasevsky, and O. Teryaev, “Accessing the gluon Wigner distribution in ultraperipheral pA collisions,” *Phys. Rev. D*, vol. 96, no. 3, p. 034009, 2017.
- [40] Y. Hatta, B.-W. Xiao, and F. Yuan, “Probing the Small- x Gluon Tomography in Correlated Hard Diffractive Dijet Production in Deep Inelastic Scattering,” *Phys. Rev. Lett.*, vol. 116, no. 20, p. 202301, 2016.
- [41] Y. Hatta, Y. Nakagawa, F. Yuan, Y. Zhao, and B. Xiao, “Gluon orbital angular momentum at small- x ,” *Phys. Rev. D*, vol. 95, no. 11, p. 114032, 2017.
- [42] Y. Hagiwara, Y. Hatta, B.-W. Xiao, and F. Yuan, “Elliptic Flow in Small Systems due to Elliptic Gluon Distributions?,” *Phys. Lett. B*, vol. 771, pp. 374–378, 2017.
- [43] X. Ji, F. Yuan, and Y. Zhao, “Hunting the Gluon Orbital Angular Momentum at the Electron-Ion Collider,” *Phys. Rev. Lett.*, vol. 118, no. 19, p. 192004, 2017.
- [44] S. Bhattacharya, A. Metz, and J. Zhou, “Generalized TMDs and the exclusive double Drell–Yan process,” *Phys. Lett. B*, vol. 771, pp. 396–400, 2017. [Erratum: *Phys.Lett.B* 810, 135866 (2020)].
- [45] S. Bhattacharya, A. Metz, V. K. Ojha, J.-Y. Tsai, and J. Zhou, “Exclusive double quarkonium production and generalized TMDs of gluons,” *Phys. Lett. B*, vol. 833, p. 137383, 2022.
- [46] D. Boer and C. Setyadi, “GTMD model predictions for diffractive dijet production at EIC,” *Phys. Rev. D*, vol. 104, no. 7, p. 074006, 2021.

- [47] D. Boer and C. Setyadi, “Probing gluon GTMDs through exclusive coherent diffractive processes,” *Eur. Phys. J. C*, vol. 83, no. 10, p. 890, 2023.
- [48] S. Bhattacharya, D. Zheng, and J. Zhou, “Accessing the gluon GTMD $F_{1,4}$ in exclusive π^0 production in ep collisions,” *Phys. Rev. D*, vol. 109, no. 9, p. 096029, 2024.
- [49] S. Bhattacharya, D. Zheng, and J. Zhou, “Probing the Quark Orbital Angular Momentum at Electron-Ion Colliders Using Exclusive π^0 Production,” *Phys. Rev. Lett.*, vol. 133, no. 5, p. 051901, 2024.
- [50] M. G. Echevarria, P. A. Gutierrez Garcia, and I. Scimemi, “GTMDs and the factorization of exclusive double Drell-Yan,” *Phys. Lett. B*, vol. 840, p. 137881, 2023.
- [51] Y. Li and H. X. Zhu, “Bootstrapping Rapidity Anomalous Dimensions for Transverse-Momentum Resummation,” *Phys. Rev. Lett.*, vol. 118, no. 2, p. 022004, 2017.
- [52] X.-D. Ji, “Off forward parton distributions,” *J. Phys. G*, vol. 24, pp. 1181–1205, 1998.
- [53] M. Diehl, “Generalized parton distributions,” *Phys. Rept.*, vol. 388, pp. 41–277, 2003.
- [54] M. Kirch, A. Manashov, and A. Schafer, “Evolution equation for generalized parton distributions,” *Phys. Rev. D*, vol. 72, p. 114006, 2005.
- [55] M. Diehl and W. Kugler, “Some numerical studies of the evolution of generalized parton distributions,” *Phys. Lett. B*, vol. 660, pp. 202–211, 2008.
- [56] V. Bertone, R. F. del Castillo, M. G. Echevarria, O. del Río, and S. Rodini, “One-loop evolution of twist-2 generalized parton distributions,” *Phys. Rev. D*, vol. 109, no. 3, p. 034023, 2024.
- [57] V. Bertone, H. Dutrieux, C. Mezrag, J. M. Morgado, and H. Moutarde, “Revisiting evolution equations for generalised parton distributions,” *Eur. Phys. J. C*, vol. 82, no. 10, p. 888, 2022.
- [58] M. G. Echevarria, I. Scimemi, and A. Vladimirov, “Unpolarized Transverse Momentum Dependent Parton Distribution and Fragmentation Functions at next-to-next-to-leading order,” *JHEP*, vol. 09, p. 004, 2016.
- [59] R. L. Jaffe and A. Manohar, “NUCLEAR GLUONOMETRY,” *Phys. Lett. B*, vol. 223, pp. 218–224, 1989.
- [60] W. Vogelsang, “ Q^2 evolution of spin dependent parton densities,” *Acta Phys. Polon. B*, vol. 29, pp. 1189–1200, 1998.
- [61] A. Bacchetta, V. Bertone, C. Bissolotti, G. Bozzi, F. Delcarro, F. Piacenza, and M. Radici, “Transverse-momentum-dependent parton distributions up to N^3 LL from Drell-Yan data,” *JHEP*, vol. 07, p. 117, 2020.
- [62] S. V. Goloskokov and P. Kroll, “Vector meson electroproduction at small Bjorken- x and generalized parton distributions,” *Eur. Phys. J. C*, vol. 42, pp. 281–301, 2005.
- [63] S. V. Goloskokov and P. Kroll, “The Role of the quark and gluon GPDs in hard vector-meson electroproduction,” *Eur. Phys. J. C*, vol. 53, pp. 367–384, 2008.
- [64] S. V. Goloskokov and P. Kroll, “An Attempt to understand exclusive π^+ electroproduction,” *Eur. Phys. J. C*, vol. 65, pp. 137–151, 2010.
- [65] B. Berthou *et al.*, “PARTONS: PARTonic Tomography Of Nucleon Software: A computing framework for the phenomenology of Generalized Parton Distributions,” *Eur. Phys. J. C*, vol. 78, no. 6, p. 478, 2018.

- [66] V. Bertone, S. Carrazza, and J. Rojo, “APFEL: A PDF Evolution Library with QED corrections,” *Comput. Phys. Commun.*, vol. 185, pp. 1647–1668, 2014.
- [67] V. Bertone, “APFEL++: A new PDF evolution library in C++,” *PoS*, vol. DIS2017, p. 201, 2018.
- [68] A. Vladimirov, V. Moos, and I. Scimemi, “Transverse momentum dependent operator expansion at next-to-leading power,” *JHEP*, vol. 01, p. 110, 2022.
- [69] M. G. Echevarria, A. Idilbi, and I. Scimemi, “Factorization Theorem For Drell-Yan At Low q_T And Transverse Momentum Distributions On-The-Light-Cone,” *JHEP*, vol. 07, p. 002, 2012.
- [70] M. Diehl, J. R. Gaunt, and P. Ploessl, “Two-loop splitting in double parton distributions: the colour non-singlet case,” *JHEP*, vol. 08, p. 040, 2021.